

Nitazoxanide Cocrystals in Combination with Succinic, Glutaric, and 2,5-Dihydroxybenzoic Acid

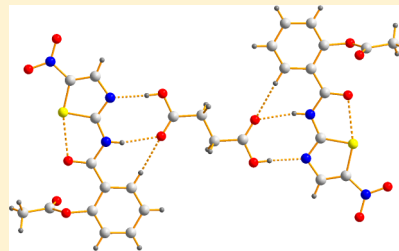
Brenda C. Félix-Sonda,[†] Jesús Rivera-Islas,[‡] Dea Herrera-Ruiz,^{*,†} Hugo Morales-Rojas,[‡] and Herbert Höpfel^{*,‡}

[†]Facultad de Farmacia, Universidad Autónoma del Estado de Morelos, Av. Universidad 1001, C.P. 62209 Cuernavaca, México

[‡]Centro de Investigaciones Químicas, Universidad Autónoma del Estado de Morelos, Av. Universidad 1001, C.P. 62209 Cuernavaca, México

Supporting Information

ABSTRACT: Combination of nitazoxanide (NTZ) with a total of 32 cocrystal formers gave cocrystals with succinic acid (NTZ-SUC, 2:1) and glutaric acid (NTZ-GLU, 1:1). Additionally, 2,5-dihydroxybenzoic acid provided a cocrystal solvate with acetonitrile (NTZ-2SDHBA-CH₃CN, 1:1:1). All solid phases were characterized by X-ray powder diffraction analysis, IR spectroscopy, thermogravimetric analysis, differential scanning calorimetry, and single-crystal X-ray diffraction analysis. Single-crystal X-ray crystallography revealed that NTZ and the carboxylic acid cocrystal formers were linked in all three cocrystals through the same supramolecular heterodimeric synthon, C(N)NH···HOOC. Despite having different stoichiometries, the crystal structures of NTZ-SUC and NTZ-GLU showed similarities in the supramolecular organization, both containing two-dimensional layers formed by NTZ molecules, which were further interconnected by single (NTZ-SUC) and homodimeric entities (NTZ-GLU) of the cocrystal former. Basic physical stability tests showed that cocrystals NTZ-SUC and NTZ-GLU are stable at least for one month under standardized temperature/relative humidity stress conditions but decompose within 1 h into the corresponding physical phase mixtures, when exposed to aqueous solutions simulating physiological gastrointestinal conditions. Measurement of the dissolution rates gave small increases of the intrinsic dissolution rate constants when compared with NTZ. Pressure stability tests showed that the cocrystals support higher pressures (at least up to 60 kg/cm²) than NTZ.



1. INTRODUCTION

Gastrointestinal parasites comprise a widespread class of living organisms including protozoa and parasitic worms (helminths). The occurrence of intestinal parasites frequently varies considerably in the diverse population groups of a country, and, as for other diseases, its prevalence is strongly coupled to the hygienic standards, health conditions, and socioeconomic status of the population. Thus, in developing countries with restrictions in the availability of safe water, wastewater treatment, and removal of refuse, the combat of intestinal parasite infections is often among the primordial health problems, and diarrhea has become the second cause of death in children below 5 years old. Worldwide, each child below four years will have 3.9 diarrhea episodes per year, and according to the World Health Organization (WHO) protozoa and helminths cause around 450 million infections each year.¹

Besides meprazine (quinacrine in the United States), the most widely prescribed antiparasitics are benzimidazole and nitroimidazole derivatives. While for meprazine side effects including skin disorders and toxic psychosis are common, the latter frequently have limitations regarding their bioavailability. Further, after prolonged use, resistance has been observed.²

Nitazoxanide (NTZ), [2-[(5-nitro-1,3-thiazol-2-yl)-carbamoyl]phenyl]ethanoate, is a commercially available nitro-thiazolyl-salicylamide ester indicated for the treatment of

gastrointestinal diseases caused by protozoa and helminthic parasites such as *Blastocystis hominis*, *Entamoeba histolytica*, *Cryptosporidium parvum*, *Giardia lamblia*, and *Trichomonas vaginalis*.^{3,4} More recently, its efficacy in the treatment of Chagas disease, rotavirus-infected pediatric patients, and chronic hepatitis B and C has been investigated.⁵ Despite being a very efficient drug, NTZ is not free of limitations, one of them being its extremely low aqueous solubility (7.55×10^{-3} mg/mL in water).⁶

To overcome solubility limitations and improve the physicochemical, biopharmaceutical, and/or pharmacotechnical specifications of an active pharmaceutical ingredient (API), the pharmaceutical industry generally explores different solid-state forms of a given API, that is, amorphous forms, polymorphs, solvates, and salts. More recently, crystal engineering techniques have been considered as additional options,⁷ and it is now well-documented that cocrystals of an API with a neutral coformer can generate solid forms with improved dissolution rates and solubility, hygroscopicity, purity, physicochemical and photostability, and pharmacotechnical specifications.^{8,9} The pharmaceutical cocrystal approach has the advantage that the number of

Received: October 25, 2013

Revised: December 18, 2013

Published: January 10, 2014

harmless potential cocrystal formers available for cocrystal formation is large,¹⁰ which is particularly relevant for APIs lacking functional groups that enable salt formation.

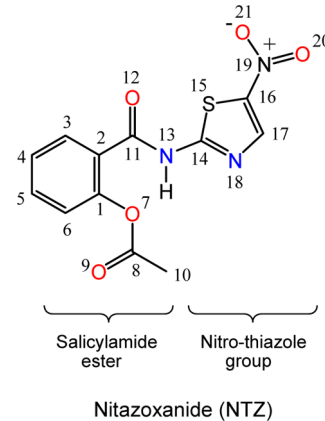
So far, little is known about the Brønsted acid–base chemistry of NTZ. In 2007, Hoffman and co-workers reported a pK_a value of 6.18, which was assigned to the deprotonation of the amide function.^{3j} However, to the best of our knowledge, data are not available for the acidity of the corresponding thiazolium cation (i.e., the conjugate weak acid of the thiazole ring in NTZ). Nevertheless, in the absence of strong electron releasing functions, thiazole derivatives are weak bases,¹¹ which diminishes the possibilities for salt formation with NTZ drastically. This is illustrated by the case of meloxicam, which is structurally somewhat related to NTZ and carries a *N*-(5-methyl-1,3-thiazol-2-yl) carboxamide instead of the *N*-(5-nitro-1,3-thiazol-2-yl)carboxamide function in NTZ. The research groups of Shan and Zaworotko have isolated and examined a total of 19 cocrystals with meloxicam using a series of different carboxylic acids with pK_a values ranging from 1.93 to 4.70.¹² Considering a pK_a value of 4.18 for meloxicam and based on the ΔpK_a rule (for $\Delta pK_a < 3$ cocrystal formation should dominate over salt formation),¹³ they proposed that salt formation involving proton transfer to the nitrogen atom of the thiazole ring will probably not occur.¹² Single-crystal diffraction and Fourier transform infrared spectroscopic analysis showed that of the 19 cocrystals¹² and three additional samples reported in successive studies,¹⁴ salt formation was observed only for the most acidic coformer malic acid ($pK_a = 1.93$), which unexpectedly ($\Delta pK_a = 2.25$) gave a cocrystal of a salt.

By virtue of the fact that NTZ has low solubility and has to be administered in relatively high doses (twice 500 mg daily for a standard treatment of 7 days),³ the discovery and identification of new solid forms of NTZ is relevant to improve its biopharmaceutical properties. So far, for NTZ only the crystal structure of one polymorph has been reported (CSD refcode: QUZWOY).¹⁵ Previous reports in the literature about approaches to improve the solubility of NTZ under physiological conditions include the development of inclusion complexes with cyclodextrines,¹⁶ the employment of hydrotropic agents,¹⁷ and solid dispersion formulations.¹⁸ Under the tested conditions, generally significant improvements of the solubility and dissolution rates (up to 12-fold) could be achieved. As a further alternative and in continuation of our current research interest in new solid phases formed with antiparasitic drugs,¹⁹ we report herein on three new solid-state phases of NTZ in the form of cocrystals with succinic, glutaric, and 2,5-dihydroxybenzoic acid, which have been characterized also by means of preliminary biopharmaceutical studies in order to evaluate if they present advantages over the drug in its actual commercially available presentations.

2. EXPERIMENTAL SECTION

2.1. Chemicals. NTZ was donated from Laboratorios Senosiain S.A de C. V., México. All cocrystal formers and solvents were commercially available from Sigma-Aldrich Company and have been used as received without further purification.

2.2. Preparative Part. Cocrystal Preparation. Liquid-assisted grinding, also known as solvent drop grinding (SDG),^{20,21} experiments were performed by mechanical grinding in a Retsch MM400 mixer mill (30 min at 25 Hz) using stainless steel grinding jars (1.5 mL). Before starting, one drop of acetonitrile, acetone, or deionized water was added to approximately 100 mg of mixtures corresponding to 2:1, 1:1, and 1:2 stoichiometric ratios of NTZ and the cocrystal former. The resulting powder was distributed on a filter paper and air-dried. For the solution-



mediated phase transformation technique (SMPT, slurry),²² NTZ and the cocrystal former were combined under stirring in the presence of 50 μL of acetonitrile. After 1 h, the sample was dried in *vacuo*. For the reaction crystallization (RC) experiments,²³ a saturated solution of the cocrystal former was prepared in acetonitrile. Upon heating to approximately 50 °C, small quantities of NTZ were added until a precipitate was observed. After precipitation was initiated, the solution was allowed to cool down to room temperature under stirring. Finally, the precipitate was filtered and air-dried.

Single-Crystal Growth. For the preparation of crystals suitable for single-crystal X-ray diffraction analysis, NTZ and the corresponding cocrystal former were dissolved in 2:1, 1:1, 1:2, 1:3, 1:4, and 1:5 stoichiometric ratios in hot acetonitrile. After filtration, small quantities of solid cocrystalline material were added, and the solutions were allowed to slowly evaporate the solvent at room temperature. Crystals suitable for single-crystal X-ray diffraction analysis were re-collected from the 1:5 (NTZ-SUC), 1:4 (NTZ-GLU), and 1:2 (NTZ-2SDHBA-CH₃CN) component mixtures, respectively.

2.3. Sample Characterization. IR Spectroscopy. IR spectra have been recorded on a NICOLET 6700 ATR spectrophotometer and measured in the range of 4000–400 cm^{-1} using the KBr pellet technique.

UV-vis Spectroscopy. UV-vis spectra have been acquired using a VARIAN UV CARY 50 spectrophotometer.

Thermogravimetric Analysis and Differential Scanning Calorimetry. Thermogravimetric-differential scanning calorimetry (TG-DSC) was performed at a heating rate of 10 °C/min within the temperature range of 30–400 °C using a current of nitrogen as inert gas purge (50 mL/min).

Powder and Single-Crystal X-ray Diffraction Analyses. Powder X-ray diffraction (PXRD) was performed in the transmission mode on a BRUKER D8-ADVANCE diffractometer equipped with a LynxEye detector ($\lambda_{\text{CuK}\alpha} = 1.5406 \text{ \AA}$, monochromator: germanium). The equipment was operated at 40 kV and 40 mA, and data were collected at room temperature in the range of $2\theta = 5\text{--}40^\circ$. Single-crystal X-ray diffraction studies were carried out on a BRUKER-APEX diffractometer equipped with a CCD area detector ($\lambda_{\text{MoK}\alpha} = 0.71073 \text{ \AA}$, monochromator: graphite). Frames were collected at $T = 293 \text{ K}$ via $\omega\phi$ -rotation at 10 s per frame (SMART).^{24a} The measured intensities were reduced to F^2 and corrected for absorption with SADABS (SAINT-NT).^{24b} Corrections were made for Lorentz and polarization effects. Structure solution, refinement, and data output were carried out with the SHELLXTL-NT program package.^{24c,d} Non-hydrogen atoms were refined anisotropically. C–H hydrogen atoms were placed in geometrically calculated positions using the riding model. O–H hydrogen atoms have been located from iterative examination of difference Fourier maps following least-squares refinements of the previous models with $d_{\text{O–H}} = 0.84 \text{ \AA}$ and $U_{\text{iso}}(\text{H}) = 1.5U_{\text{eq}}(\text{O})$. In NTZ-SUC, the asymmetric unit consists of one NTZ molecule and half a molecule of SUC, since the cocrystal former is located on a crystallographic inversion center. Simulated PXRD patterns and hydrogen-bonding interactions in the crystal lattice were calculated with the WINGX program package.²⁵ DIAMOND was used for the creation of figures.²⁶ Crystallographic data

Table 1. Results of the Screening Experiments for the Formation of Cocrystals with Nitazoxanide Using Aliphatic Dicarboxylic Acids

Cocrystal Former	CH ₃ CN	H ₂ O	C ₃ H ₆ O	Cocrystal Former	CH ₃ CN	H ₂ O	C ₃ H ₆ O	Cocrystal Former	CH ₃ CN	H ₂ O	C ₃ H ₆ O
Oxalic acid 	x	x	x	Glycolic acid 	x	x	x	Malonic acid 	x	x	x
Succinic acid 	✓	✓	✓	Fumaric acid 	x	x	x	Maleic acid 	x	x	x
D,L-Malic acid 	x	x	x	L-Malic acid 	x	x	x	D-Malic acid 	x	x	x
D,L-Tartaric acid 	x	x	x	D-Tartaric acid 	x	x	x	Glutaric acid 	✓	✓	✓
Adipic acid 	x	x	x	Pimelic acid 	x	x	x	Suberic acid 	x	x	x
Azelaic acid 	x	x	x	Sebacic acid 	x	x	x	Citric acid 	x	x	x

for the three crystal structures have been deposited with the Cambridge Crystallographic Data Centre as supplementary publications no. CCDC-968558–968560. Copies of the data can be obtained free of charge on application to CCDC, 12 Union Road, Cambridge CB2 1EZ, UK (fax: (+44)1223-336-033; e-mail: deposit@ccdc.cam.ac.uk, www:<http://www.ccdc.cam.ac.uk>).

2.4. Biopharmaceutical Assays. Physical Phase Stability Tests. Twenty-five milligram samples of NTZ-SUC, NTZ-GLU, or NTZ-2SDHBA-CH₃CN were added to a screw-capped vial containing 4 mL of either deionized water, 0.1 N HCl adjusted to pH 1.2, or phosphate buffer (pH 7.5, 3% w/v CTAB). The resulting suspensions were stirred at room temperature for different time periods (1, 3, 6, 12, 24, 48, and 72 h) and, after filtration, examined by PXRD analysis. All experiments were carried out in triplicate.

Indicative Stability Tests. Thirty milligram samples of NTZ-SUC, NTZ-GLU, or NTZ-2SDHBA-CH₃CN were placed in glass vials and kept in humidity-controlled chambers for 4 weeks under the following conditions: 40 °C/0% RH (REVCO, RI-23-1060-ABA), 50 °C/0% (RIOS ROCHA, EOS1), and 40 °C/75% RH (BINDER, IP 20). After 4 weeks, the solids were analyzed by PXRD analysis. All experiments were carried out in duplicate.

Intrinsic Dissolution Rate. Samples (150 mg) of NTZ, NTZ-SUC, or NTZ-GLU were compressed into a disk with a surface area of 0.5 cm² using a hydraulic press (GlaxoSmithKline Beecham, N0405 CIA24) at a total force of 30 kg/cm² (10 s). The resulting products were subsequently analyzed in Wood's apparatus (VARIAN, VK7010) and rotated at 100 rpm in 300 mL of a vacuum-filtered and degassed medium (phosphate buffer, pH = 7.5, containing 3% w/v CTAB) at 37 °C. Experiments were carried out in triplicate. Aliquots of dissolution samples (3 mL) were taken at intervals of 5, 10, 15, 30, 60, 90, 120, 180, 240, 300, and 360 min and analyzed by UV-vis spectroscopy at a wavelength of 435 nm. The amount of NTZ dissolved in the dissolution rate determinations was derived from a previously established calibration curve for NTZ (*r* = 0.999). For the generation of this curve, the cocrystal formers SUC and GLU were not considered, since both reagents did not absorb in this region. Each volume sample extracted from the dissolution experiment (from different timing) was replaced with an equal volume of fresh medium (3 mL). The resulting

dissolution profiles were generated using the ORIGIN PRO 8.1 software package.

Pressure Tests. Samples (150 mg) of NTZ, NTZ-SUC, or NTZ-GLU were treated for 10 s with a hydraulic press (GlaxoSmithKline Beecham, N0405 CIA24) at total forces of 30, 35, 40, 50, and 60 kg/cm² and then visually examined to establish solid performance.

3. RESULTS AND DISCUSSION

3.1. Screening Experiments and PXRD Analysis. With the hypothesis that the carboxamidine function of NTZ might have a propensity to form heterodimeric synthons with COOH groups (see section 3.4), we selected mainly carboxylic acids for the screening experiments in the search of cocrystalline phases with NTZ. Because of the observation that NTZ possesses only one moderately strong hydrogen bond donor site (NH group) but four such hydrogen bond acceptor sites (N_{thiazole}, OAc, C=O_{amide}, and NO₂ groups), our series of potential cocrystal formers included carboxylic acids having preferentially two or more O–H donor sites. Thus, mostly aliphatic dicarboxylic acids and aromatic hydroxybenzoic acids have been selected for the screening process.

Screening experiments were performed with a total of 32 cocrystal formers using the solvent drop grinding method.^{20,21} Three solvents of different polarities were employed: acetone, acetonitrile, and water. Initially, NTZ and the corresponding cocrystal former were combined in 1:1 stoichiometric ratios. The resulting products were then analyzed by PXRD analysis and to discriminate cocrystalline phases from polymorphs or solvates, parallel grinding experiments using only NTZ or the corresponding cocrystal former were performed. Analysis of the PXRD patterns revealed that novel solid phases of NTZ have been achieved with succinic acid (NTZ-SUC), glutaric acid (NTZ-GLU), and 2,5-dihydroxybenzoic acid (NTZ-2SDHBA-CH₃CN). In order to establish the NTZ–cocrystal former stoichiometry of the cocrystalline phases, subsequent mechanical

Table 2. Results of the Screening Experiments for the Formation of Cocrystals with Nitazoxanide Using Benzoic Acid, Hydroxy- and Aminobenzoic Acids, Hydroquinone, and Nicotinamides

Cocrystal Former	CH ₃ CN	H ₂ O	C ₃ H ₆ O	Cocrystal Former	CH ₃ CN	H ₂ O	C ₃ H ₆ O	Cocrystal Former	CH ₃ CN	H ₂ O	C ₃ H ₆ O
Benzoic acid				2-Hydroxybenzoic acid				3-Hydroxybenzoic acid			
	x	x	x		x	x	x		x	x	x
4-Hydroxybenzoic acid				3-Aminobenzoic acid				2,3-Dihydroxybenzoic acid			
	x	x	x		x	x	x		x	x	x
2,4-Dihydroxybenzoic acid				2,5-Dihydroxybenzoic acid				2,6-Dihydroxybenzoic acid			
	x	x	x		✓	x	x		x	x	x
3,4-Dihydroxybenzoic acid				3,5-Dihydroxybenzoic acid				Hydroquinone			
	x	x	x		x	x	x		x	x	x
Nicotinamide				Isonicotinamide							
	x	x	x		x	x	x				

grinding experiments using 2:1 and 1:2 NTZ–cocrystal former stoichiometric ratios were carried out. Comparative examination of the corresponding PXRD patterns of NTZ, the respective cocrystal former, and the solids obtained from the grinding experiments in the different stoichiometric ratios indicated that GLU generated 1:1 cocrystals, while SUC gave 2:1 specimens and 2SDHBA a 1:1:1 cocrystal solvate with acetonitrile. The cocrystalline phase with 2SDHBA could be obtained only when using acetonitrile as solvent in the liquid-assisted grinding process, and subsequent thermogravimetric analysis revealed that this phase was indeed a cocrystal solvate (*vide infra*). All further relevant details of the screening experiments are summarized in Tables 1 and 2.

Figure 1a–c shows the PXRD patterns of NTZ, GLU, and the solid from the 1:1 grinding experiment with CH₃CN. The diffractograms of the solids resulting from the 2:1 and 1:2 grinding experiments show peaks of unreacted NTZ in the first case and peaks of unreacted GLU in the latter case (Figure S1, Supporting Information), while the PXRD pattern for the 1:1 combination of NTZ and GLU does not contain peaks of residual starting materials (Figure 1c). On the contrary, in the case of the solids formed from the reaction of NTZ with SUC, the diffractograms of the 1:1 and 1:2 assays both contain peaks of unreacted SUC, which would be expected for a 2:1 composition (Figure S2, Supporting Information). On the basis of the same procedure, for the novel solid phase with 2SDHBA a 1:1 composition was established (Figure S3, Supporting Information). In all cases, the proposed cocrystal compositions were confirmed by single-crystal X-ray diffraction analysis, and the PXRD patterns simulated from the single-crystal data were in

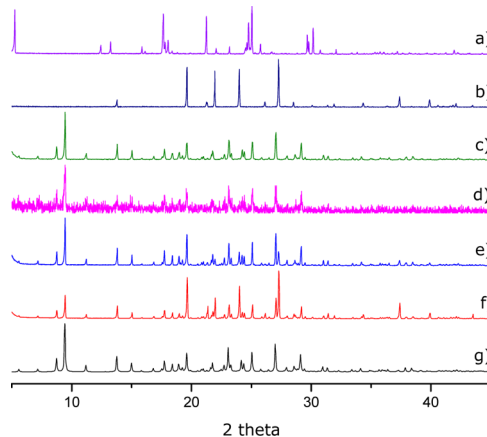


Figure 1. PXRD patterns of the following samples and experiments: (a) NTZ, (b) GLU, (c) NTZ-GLU prepared by SDG with acetonitrile using 1:1 stoichiometry, (d) NTZ-GLU prepared by neat grinding using 1:1 stoichiometry, (e) NTZ-GLU prepared by SMPT in acetonitrile, (f) NTZ-GLU prepared by RC in acetonitrile, (g) pattern of NTZ-GLU simulated from the single-crystal X-ray diffraction analysis.

good agreement with the experimentally observed diffractograms of the corresponding cocrystalline powders (Figures 1–3).

Of the three cocrystalline phases, NTZ-GLU is the most robust, since it can be prepared by different further preparative methods including mechanical grinding in the absence of solvent (neat grinding), solution-mediated phase transformation (SMPT, slurry technique),²² and reaction crystallization (RC).²³ Figure 1d–f provides an overview of the PXRD patterns

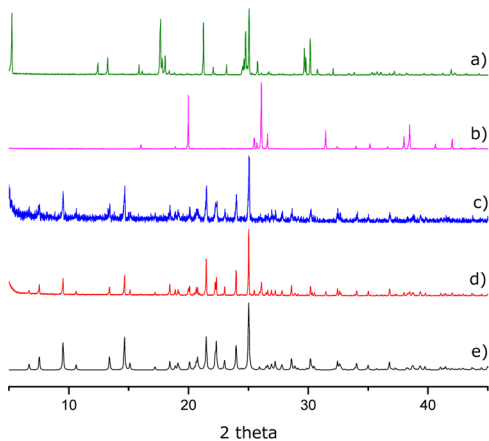


Figure 2. PXRD patterns of the following samples and experiments: (a) NTZ, (b) SUC, (c) NTZ-SUC prepared by SDG with acetonitrile using 2:1 stoichiometry, (d) NTZ-SUC prepared by SMPT in acetonitrile, (e) pattern of NTZ-SUC simulated from the single-crystal X-ray diffraction analysis.

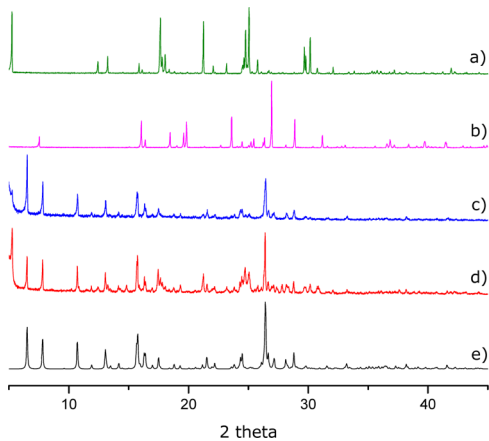


Figure 3. PXRD patterns of the following samples and experiments: (a) NTZ, (b) 2SDHBA, (c) NTZ-2SDHBA-CH₃CN prepared by SDG with acetonitrile using 1:1 stoichiometry, (d) NTZ-2SDHBA-CH₃CN prepared by SMPT in acetonitrile, (e) pattern of NTZ-2SDHBA-CH₃CN simulated from the single-crystal X-ray diffraction analysis.

of the products obtained for NTZ-GLU by each technique, which all agree with the pattern simulated from the single-crystal X-ray diffraction analysis (Figure 1g). On the contrary, cocrystals NTZ-SUC and NTZ-2SDHBA-CH₃CN could be obtained only in the presence of solvent using either the SDG or SMPT technique. Moreover, for NTZ-2SDHBA-CH₃CN heating of the cocrystal solvate to 80 °C for 15 min causes decomposition, giving a phase mixture of the starting materials.

Cocrystals with either succinic, glutaric, or 2,5-dihydroxy benzoic acid also have been obtained previously with AMG 517,²⁷ carbamazepine,²⁸ itraconazole,²⁹ meloxicam,¹² piroxicam,³⁰ praziquantel,¹⁹ theophylline,³¹ among others.³²

3.2. IR Spectroscopy. Comparison of the solid-state IR spectra of NTZ, the cocrystal former, and the corresponding cocrystal (NTZ-SUC, NTZ-GLU, and NTZ-2SDHBA-CH₃CN) allows us to confirm that new solid forms have been generated.^{19,33} This is illustrated for NTZ-GLU in Figure 4, showing that the IR spectrum of the cocrystal does not correspond to a superposition of the IR spectra of the individual components (NTZ and GLU). The analogous graphs for cocrystals NTZ-SUC and NTZ-2SDHBA-CH₃CN are available

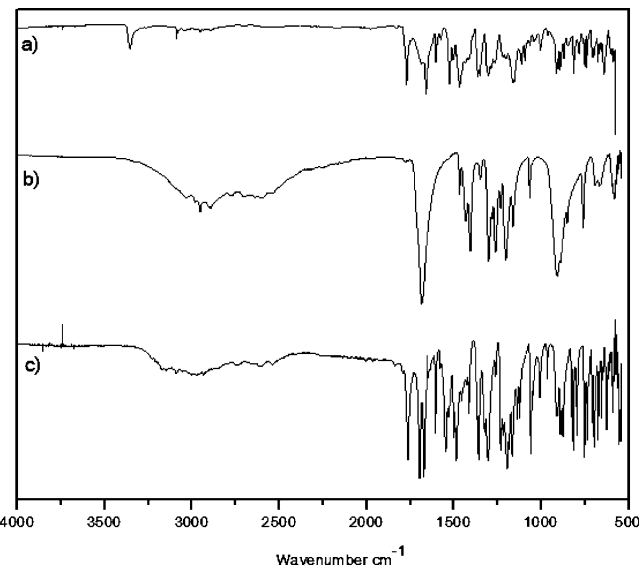


Figure 4. IR spectra of (a) NTZ, (b) GLU, and (c) NTZ-GLU.

in the Supporting Information (Figures S4–S5). Listings of relevant IR bands for NTZ and the corresponding cocrystal formers are given in Table 3.

When compared to the individual components of the cocrystal, the displacements of the vibrational bands provide also some information on the intermolecular binding interactions in the cocrystal lattice. As indicated in Table 3, the most characteristic bands in the IR spectrum of NTZ appear at 3355 cm⁻¹ for the NH stretching vibration, at 1771 cm⁻¹ for the ester function, at 1660 and 1525 cm⁻¹ for vibrations of the amide group (amide I and II), of which the latter is expected to overlap with the band resulting from the symmetric stretching vibration of the nitro group, and at 1362 cm⁻¹ for the asymmetric ν_{NO_2} stretching vibration.¹⁵ For the cocrystal formers, the most notable band corresponds to the $\nu_{C=O}$ vibration of the carboxyl groups, in the range of 1656 to 1684 cm⁻¹. All three cocrystalline phases gave broad bands in the range of 2500–3500 cm⁻¹, which are different from those observed for the starting materials and indicative of significant changes in the supramolecular hydrogen bonding network.³⁴ This is also illustrated by the shift of the ν_{N-H} stretching vibrations of NTZ to lower wavenumbers and shift displacements of the vibrations originated from the above-mentioned remaining hydrogen bond donor and acceptor sites (Table 3). For NTZ-2SDHBA-CH₃CN, the presence of acetonitrile in the solid phase is evidenced by a band at 2271 cm⁻¹ for the vibration of the nitrile group.

The absence of an intense band in the range of 1550–1610 cm⁻¹, which is the region characteristic for the asymmetric vibration of arylcarboxylate ions, eliminates the possibility of salt formation.³⁴

3.3. DSC-TG Analysis. Figure 5 shows the TG profiles of cocrystals NTZ-SUC, NTZ-GLU, and NTZ-2SDHBA-CH₃CN in comparison to the curve of pure NTZ. The corresponding individual TG-DSC profiles are given in Figures S6–S9, Supporting Information. The most relevant data from the TG-DSC analysis are condensed in Table 4.

Figure S6 (Supporting Information) indicates that NTZ melts at 202 °C and starts to decompose at this temperature. Cocrystals NTZ-SUC and NTZ-GLU are thermally less stable than NTZ and weight loss initiates at approximately 150 and 120 °C, respectively. However, melting before decomposition is only

Table 3. Relevant Bands in the IR Spectra of NTZ, NTZ-SUC, NTZ-GLU, NTZ-2SDHBA-CH₃CN, and the Respective Cocrystal Formers (cm⁻¹)

	NTZ	SUC	GLU	2SDHBA	NTZ-SUC	NTZ-GLU	NTZ-2SDHBA-CH ₃ CN
$\tilde{\nu}_{\text{O-H, N-H}}$	3355 3088	2626 2530	2894 2603	3073	3236 3211 3180 3084	3228 3211 3174 3146 3112 3092	3317 3158 3102
$\tilde{\nu}_{\text{amide I}}$	1660				1677/1692	1672/1697	1660/1694
$\tilde{\nu}_{\text{amide II}}$	1525				1547/1527	1547/1531	1549/1529
$\tilde{\nu}_{\text{C=O (ester)}}$	1771				1772	1763	1753
$\tilde{\nu}_{\text{C=O(carboxyl group)}}$		1675	1684	1656	1677/1692	1672/1697	1660/1694
$\tilde{\nu}_{\text{nitro}}$	1525 1362				1547/1527 1354	1547/1531 1358	1549/1529 1357

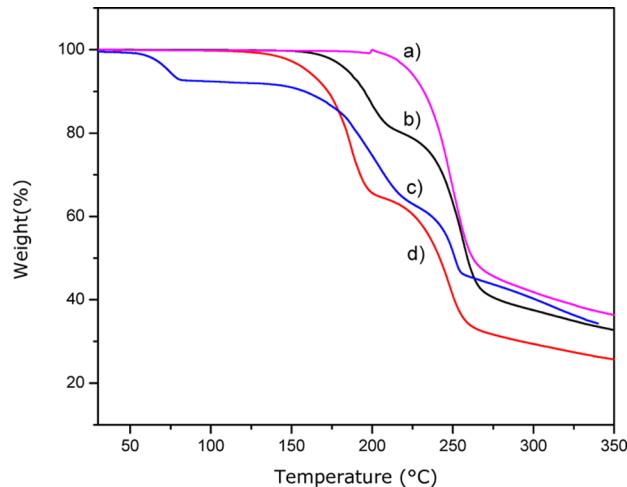


Figure 5. Comparison of the TG profiles of (a) NTZ, (b) NTZ-SUC, (c) NTZ-2SDHBA-CH₃CN, and (d) NTZ-GLU.

observed for NTZ-GLU with an extrapolated onset temperature of 141 °C. Analysis of the weight loss for the thermal event in the temperature range of 150–215 °C for NTZ-SUC and 120–205 °C for NTZ-GLU indicates that the decomposition due to heating corresponds mainly to the elimination of the cocrystal former (0.50 stoichiometric equivalents in the case of NTZ-SUC), followed by degradation of NTZ at temperatures that are close to those observed for pure NTZ (Table 4). Nevertheless, there is a significant difference between the experimental and calculated weight losses for the cocrystal former elimination indicating that this process also catalyzes the decomposition of NTZ.

As expected, the cocrystal solvate NTZ-2SDHBA-CH₃CN shows three thermal events. First, loss of CH₃CN in the temperature range of 65–85 °C, followed by evaporation of 2SDHBA in the range of 150–220 °C, and, finally, decomposition of NTZ initiating at an extrapolated onset temperature of 257 °C. Contrary to NTZ-SUC and NTZ-GLU, for this cocrystal solvate the experimental and calculated weight

Table 4. Relevant Data from the DSC-TG Analyses of NTZ, Cocrystals NTZ-SUC, NTZ-GLU, NTZ-2SDHBA-CH₃CN, and the Respective Cocrystal Formers

compound	NTZ/coformer/ MeCN ratio	coformer		NTZ and cocrystals			thermal process
		peak temp ^a [°C]	onset temp ^a [°C]	peak temp [°C]	onset temp [°C]	% weight loss [°C] (exper/calcd)	
NTZ				205 (m.p.) 259	202 (m.p.) 247	— 47.0/—	degradation of NTZ ^b
NTZ-SUC	2:1	191 (m.p.)	189 (m.p.)	190	183	19.3/16.1 ^d	coformer elimination
		218 ^c	206 ^c	258	248	37.4/—	degradation of NTZ ^b
NTZ-GLU	1:1	101 (m.p.) 217 ^c	99 (m.p.) 198 ^c	147 180	141 165	— 35.0/30.1 ^d	melting coformer elimination
				257	248	29.3/—	degradation of NTZ ^b
NTZ-2SDHBA-MeCN	1:1:1	207 ^c	205 ^c	83	66	8.2/8.2	solvent evaporation
				178	176	29.4/30.7	coformer elimination
				260	257	17.7/—	degradation of NTZ ^b

^aDetermined by DSC heat flow at an altitude of 1800 m above sea level. ^bThe indicated experimental weight loss refers to the first step of degradation. Weight losses could not be calculated since the products of the pyrolysis are unknown. ^cCoformer sublimes. ^dApparently, the cocrystal former catalyzes the degradation of NTZ as indicated by the larger than expected weight loss for the cocrystal former elimination process.

Scheme 1. (a) Primordial Intra- and Intermolecular Interactions in the Crystal Structure of NTZ and (b) Motifs of the Principal Intra- and Intermolecular Interactions in the Crystal Structures of Cocrystals NTZ-SUC, NTZ-GLU, and NTZ-25DHBA-CH₃CN

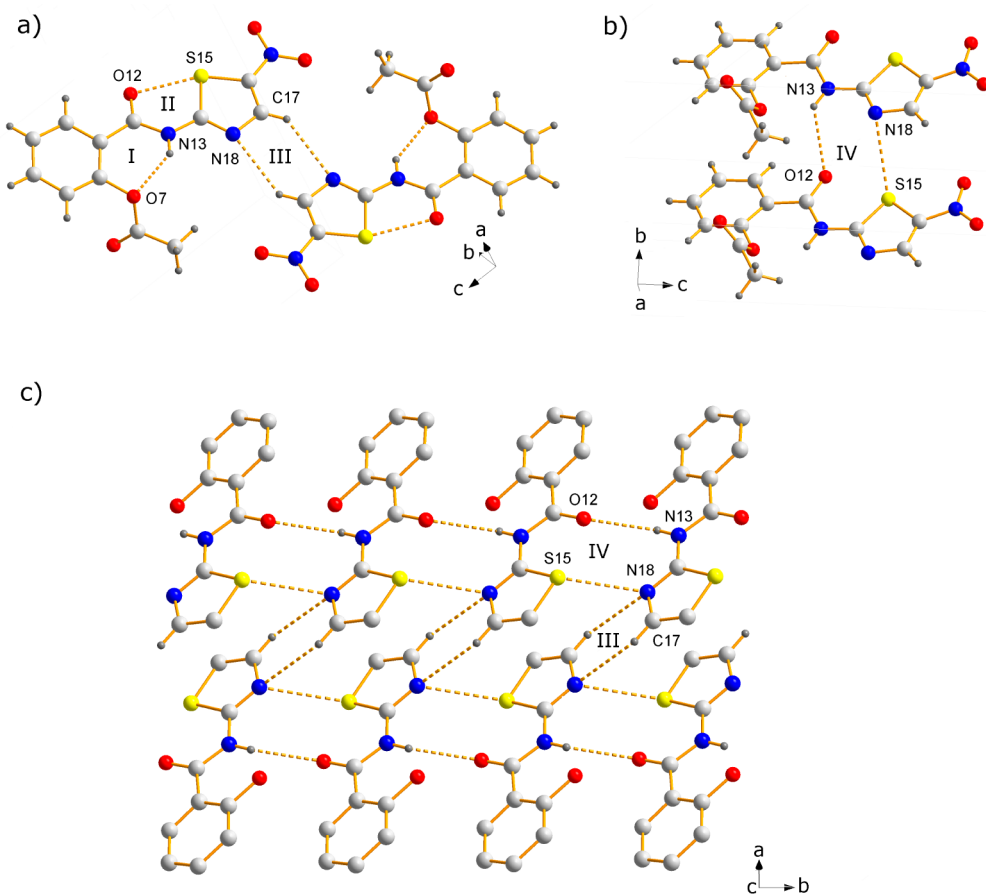
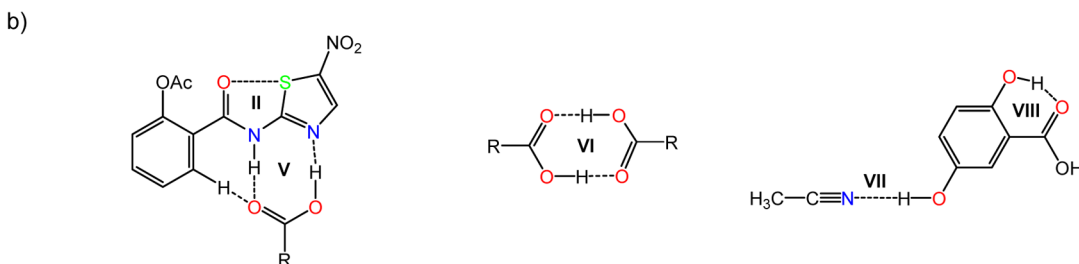
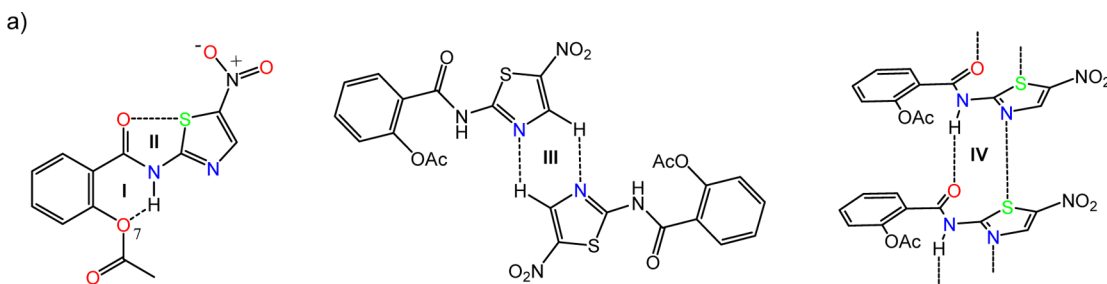


Figure 6. Fragments of the crystal structure of NTZ, showing the homodimeric motifs III and IV (a, b) and the formation of 1D double chains parallel to *b* (c). Note: For clarity, in panel (c) part of the atoms have been omitted.

losses for the evaporation of the cocrystal former are in excellent agreement (29.4/30.7%).

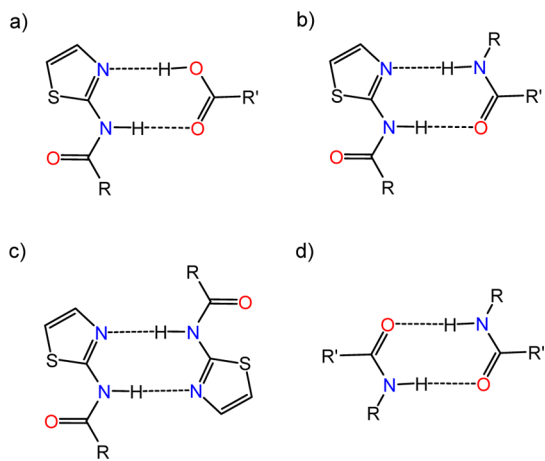
3.4. Single-Crystal X-ray Diffraction Analysis. In order to facilitate a proper selection of possible cocrystal formers for

NTZ, before starting with the screening experiments, we examined the supramolecular interactions in the previously reported crystal structure of the only polymorph known so far for this API.¹⁵ In this crystal structure, NTZ crystallized with two

crystallographically independent molecules in the asymmetric unit. The two molecules have similar conformations with characteristic intramolecular N–H···OAc hydrogen bonds and S···O interactions (motifs I and II, Scheme 1). Within the crystal lattice, each of two independent NTZ molecules formed homodimeric aggregates through C–H···N interactions between the thiazolyl groups (motif III, Figure 6a). The dimeric entities are further linked through N–H_{amide}···O=C_{amide} (N–H = 0.88 Å; H···O = 2.66 and 2.70 Å, N···O = 3.264(2) and 3.281(2) Å, N–H···O = 124 and 126°) and N_{thiazole}···S_{thiazole} (3.267(2) and 3.283(2) Å) interactions (motif IV in Scheme 1, Figure 6b) along axis *b* to give one-dimensional (1D) double chains parallel to *b* (Figure 6c). The geometric parameters of the N–H_{amide}···O=C_{amide} hydrogen bonds indicate that these interactions are relatively weak, in agreement with the presence of intramolecular N–H···O hydrogen bonding (N–H = 0.88 Å; H···O = 2.01 and 2.04 Å, N···O = 2.681(2) and 2.700(2) Å, N–H···O = 131 and 132°). Reports on O···S and N···S interactions are still relatively rare, although theoretical calculations have provided conclusive evidence for their existence.^{33,35} Overall, each NTZ molecule participates in a total of four N–H···O=C and N···S interactions. The supramolecular interaction pattern of the crystal structure is accomplished by an additional series of intermolecular C–H···O and π···π contacts.

This analysis reveals that the carboxamidine fragment in NTZ might be the most adequate binding site for the formation of a reliable supramolecular synthon with the purpose of cocrystal formation. The underlying RC(=N)NHR entity also comprises the essential section for the hydrogen bonding capabilities of 2-aminopyridines, which have been explored previously in crystal engineering.³⁶ Previous reports on cocrystals with other APIs containing *N*-(1,3-thiazol-2-yl)carboxamide or related functionalities have shown that the carboxamidine fragment can give heterodimeric hydrogen bonding motifs with cocrystal formers containing carboxylic acids and carboxamides (Scheme 2a,b).^{12,14,27,30,33,37} A search of the Cambridge Structural Database (CSD version 5.34)³⁸ for crystal structures containing simultaneously a *N*-(1,3-thiazol-2-yl)carboxamide and a carboxylic acid group revealed a total of nine entries, which all correspond to cocrystalline phases with meloxicam.^{12,14} All of

Scheme 2. Heterodimeric Synthons Formed between the *N*-(1,3-Thiazol-2-yl)carboxamide Functionality and a (a) Carboxylic Acid or (b) Carboxamide Group and Homodimeric Motifs Formed between (c) *N*-(1,3-Thiazol-2-yl)carboxamide and (d) Carboxamide Groups



these contained the heterodimeric synthon shown in Scheme 2a, and only in one case salt formation was observed according to proton transfer from the COOH group to the thiazole nitrogen. However, an analogous search for crystal structures containing the *N*-(1,3-thiazol-2-yl)carboxamide group and an additional carboxamide function provided eight entries, of which only one (13%) corresponded to the heterodimeric synthon given in Scheme 2b. Three entries (38%) contained the carboxamidine homodimer synthon (Scheme 2c) and a further sample the carboxamide homodimer (Scheme 2d). Nevertheless, none of these eight entries corresponded to a cocrystalline phase, but all were single-component structures.

The cocrystal growth from solution of APIs having low solubility frequently requires an excess of the cocrystal former and addition of small quantities of solid cocrystalline material (seeding).^{19,33,39} Accordingly, for the growth of single cocrystals with NTZ, the drug and the corresponding cocrystal formers were dissolved in 2:1, 1:1, 1:2, 1:3, 1:4, and 1:5 stoichiometric ratios in hot acetonitrile. After filtration and addition of a small quantity of the previously obtained cocrystalline phase, the resulting solvents were allowed to slowly evaporate the solvent at room temperature. This procedure provided cocrystals suitable for single-crystal X-ray diffraction analysis for NTZ-SUC, NTZ-GLU, and NTZ-25DHBA-CH₃CN and enabled us a comparative structural analysis (for more details see Experimental Section). The cocrystals had significantly distinct morphologies between each other and when compared to NTZ. Additionally, the cocrystals of NTZ-25DHBA-CH₃CN were yellow (Figure 7).

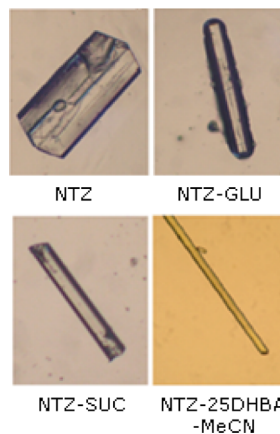


Figure 7. Crystals of NTZ and its cocrystals with SUC, GLU, and 25DHBA, which can be distinguished by their different morphologies.

The most relevant crystallographic data for NTZ-SUC, NTZ-GLU, and NTZ-25DHBA-CH₃CN are listed in Table 5, and for the purpose of comparison the previously reported data for pure NTZ have been also included.¹⁵ The motifs of the principal intra- and intermolecular interactions in NTZ-SUC, NTZ-GLU and NTZ-25DHBA-CH₃CN are represented in Scheme 1. The corresponding geometric parameters are summarized in Table 6. Further relevant interactions are given in Table S1, Supporting Information.

Cocrystals NTZ-SUC (2:1) and NTZ-GLU (1:1). NTZ-SUC crystallized in the monoclinic space group *P*2₁/*n*, but for the sake of a better comparison with the data of NTZ-GLU, the data were transformed to space group *P*2₁/*c*. In NTZ-SUC, the asymmetric unit comprises one crystallographically independent NTZ molecule and half a molecule of the cocrystal former which is localized on a crystallographic inversion center, whereas the

Table 5. Crystallographic Data for Compounds NTZ, NTZ-SUC, NTZ-GLU, and NTZ-2SDHBA-CH₃CN

crystal data ^a	NTZ ^b	NTZ-SUC (2:1)	NTZ-GLU (1:1)	NTZ-2SDHBA-CH ₃ CN (1:1)
formula	C ₁₂ H ₉ N ₃ O ₅ S	2C ₁₂ H ₉ N ₃ O ₅ S·C ₄ H ₆ O ₄	C ₁₂ H ₉ N ₃ O ₅ S·C ₅ H ₈ O ₄	C ₁₂ H ₉ N ₃ O ₅ S·C ₇ H ₆ O ₄ ·CH ₃ CN
MW (g mol ⁻¹)	307.28	366.33	439.40	502.45
space group	Pna2 ₁	P2 ₁ /c	P2 ₁ /c	P̄1
<i>a</i> (Å)	14.302(2)	16.770(5)	12.370(4)	7.5051(14)
<i>b</i> (Å)	5.2800(8)	5.0216(15)	5.0586(15)	11.468(2)
<i>c</i> (Å)	33.183(5)	23.582(8)	31.715(9)	13.694(2)
α (deg)	90	90	90	83.123(3)
β (deg)	90	128.077(6)	94.495(6)	84.660(3)
γ (deg)	90	90	90	82.833(4)
<i>V</i> (Å ³)	2505(8)	1563.2(8)	1978.5(10)	1157.3(4)
<i>Z</i> (<i>Z'</i>)	8 (2)	2 (0.5)	4 (1)	2 (1)
μ (mm ⁻¹)	0.286	0.253	0.220	0.200
ρ_{calcd} (g cm ⁻³)	1.628	1.557	1.475	1.442
<i>R</i> ^{c,d}	0.0307	0.0743	0.0699	0.0657
<i>R</i> _w ^{e,f}	0.0799	0.1658	0.1637	0.1328
GOF	1.046	1.085	1.018	1.037

^a $\lambda_{\text{MoK}\alpha} = 0.71073 \text{ \AA}$. ^bData from ref 15. ^c $F_o > 4\sigma(F_o)$. ^d $R = \sum|F_o| - |F_c|/\sum|F_o|$. ^eAll data. ^f $R_w = [\sum w(F_o^2 - F_c^2)^2/\sum w(F_o^2)^2]^{1/2}$.

Table 6. Geometric Parameters for the Principal Intra- and Intermolecular Interactions in NTZ and Cocrystals NTZ-SUC, NTZ-GLU, and NTZ-2SDHBA-CH₃CN

compound	motif	interaction	D–H [Å]	H···A [Å]	D···A [Å]	$\angle\text{DHA}$ [deg]	symmetry code
NTZ ^a	I	N13–H13···O7	0.88	2.04	2.700(2)	131	+x, +y, +z
			0.88	2.01	2.681(2)	132	+x, +y, +z
	II	O12···S15			2.618(2)		+x, +y, +z
					2.641(2)		+x, +y, +z
	III	C17–H17···N18	0.95	2.74	3.541(2)	142	−x + 1, −y, +z−1/2
			0.95	2.74	3.537(2)	142	−x + 1, −y, +z + 1/2
	IV	N13–H13···O12	0.88	2.70	3.281(2)	124	+x, +y − 1, +z
			0.88	2.66	3.264(2)	126	+x, +y + 1, +z
					2.578(5)		+x, +y, +z
							+x, +y − 1, +z
NTZ-SUC	II	O12···S15					+x, +y + 1, +z
	V	N13–H13···O24	0.84	2.09	2.910(5)	167	+x, +y − 1, +z
	V	O22–H22···N18	0.84	1.93	2.766(5)	174	+x, +y + 1, +z
	V	C3–H3···O24	0.93	2.31	3.224(6)	167	+x, +y − 1, +z
NTZ-GLU	II	O12···S15			2.626(3)		+x, +y, +z
	V	N13–H13···O24	0.84	2.12	2.954(4)	169	+x − 1, +y + 1, +z
	V	O22–H22···N18	0.84	1.86	2.693(4)	171	+x + 1, +y − 1, +z
	V	C3–H3···O24	0.93	2.33	3.219(5)	161	+x − 1, +y + 1, +z
	VI	O29–H29···O30	0.84	1.80	2.640(4)	174	−x + 1, −y, −z
NTZ-2SDHBA	II	O12···S15			2.692(2)		+x, +y, +z
	V	N13–H13···O24	0.84	2.00	2.837(3)	177	−x + 1, −y, −z + 2
	V	O22–H22···N18	0.84	1.88	2.719(3)	174	−x + 1, −y, −z + 2
	V	C3–H3···O24	0.93	2.70	3.185(4)	113	−x + 1, −y, −z + 2
	VII	O31–H31···N35	0.84	2.00	2.828(4)	171	−x + 1, −y + 1, −z + 1
	VIII	O27–H27···O24	0.84	1.86	2.617(3)	150	+x, +y, +z

^aData from ref 15, but atoms are numbered analogous to the NTZ molecules of the cocrystals described herein. The asymmetric unit comprises two crystallographically independent molecules.

asymmetric unit of NTZ-GLU is composed only of each one NTZ and one cocrystal former molecule. This confirms the results from the PXRD analysis, which gave 2:1 and 1:1 stoichiometries, respectively, and is also illustrated by the comparison of the simulated and experimental PXRD patterns (Figure 2c,e for NTZ-SUC; Figure 1c,g for NTZ-GLU).

Within the crystal lattice of NTZ-SUC, each succinic acid is hydrogen bonded to two NTZ molecules, forming adducts with crystallographic inversion symmetry of the composition NTZ-SUC-NTZ. The underlying heterodimeric hydrogen bonding motif V is formed between the COOH group of the cocrystal former and the carboxamidine entity of the API molecule and is

additionally reinforced by a C–H···O contact with the aromatic ring of the salicylamide ester moiety (Scheme 1b, Figure 8a). On the contrary, in NTZ-GLU only one COOH group of the dicarboxylic acid is involved in the heterodimeric hydrogen bonding motif V, while the second participates in a homodimeric COOH···HOOC synthon (motif VI, Scheme 1b) with a neighboring GLU molecule. Thus, in this case [2 + 2] aggregates are generated (Figure 8b). A similar behavior has been observed previously by Zaworotko and co-workers for meloxicam cocrystals with GLU and SUC.¹² Similarly, for cocrystals of AMG 517 with malonic and succinic acid, Bak and co-workers

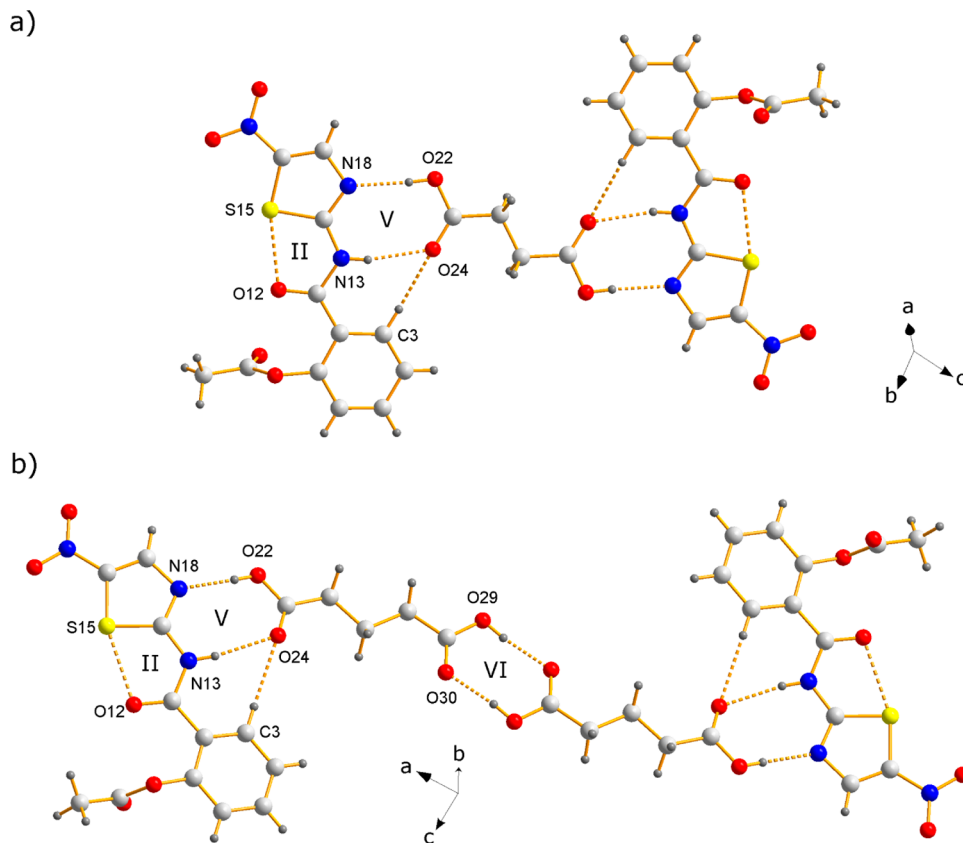


Figure 8. Fragments of the crystal structures of NTZ-SUC and NTZ-GLU, showing the presence of [2 + 1] aggregates in the first case (a) and [2 + 2] aggregates in the second case (b).

observed the formation of [2 + 2] and [2 + 1] adducts, respectively.⁴⁰

Comparison of NTZ-SUC and NTZ-GLU shows that in both crystal structures the NTZ molecules are connected similarly to give in the first instance 1D supramolecular chains along *b*. The relatively weak intermolecular contacts within these chains correspond to two C–H…O, one π…π, and one O…C interaction. Of these, the O…C interaction occurs between the OAc oxygen and the carbon of the amide moiety. The π…π contact is formed between two carbon atoms (C3 and C6) of neighboring NTZ molecules (Table S1, Figure S10a,b, Supporting Information). These 1D chains are linked to 2D layers with the difference that in NTZ-SUC neighboring chains are related only by translational symmetry, while in NTZ-GLU the symmetry relationship corresponds to *c*-glide reflection. The three-dimensional (3D) supramolecular structures are accomplished by interconnection of the 2D layers through the cocrystal former entities, consisting of single SUC molecules in the first case and GLU-GLU aggregates in the second case (Figure 9). In NTZ-SUC, neighboring NTZ layers are connected additionally by C–H…N hydrogen bonds giving an overall 3D NTZ network. As can be seen from Figure 8, the mutual spatial orientation of the terminal coordinating COOH groups in the cocrystal former spacer groups in NTZ-SUC and NTZ-GLU is similar, which due to the odd–even effect would not be the case if GLU would act as a single-molecule spacer. Thus, these structures provide a further example showing that neighboring members within the homologous series of aliphatic dicarboxylic acids can actuate quite differently in a supramolecular organization process.⁴¹ Nevertheless, there are other examples of cocrystals in which neighboring members of the homologous series of aliphatic

dicarboxylic acids gave isomorphous or structurally closely related crystal structures.^{28b,42}

Cocrystal Solvate NTZ-25DHBA-CH₃CN (1:1:1). Contrary to succinic and glutaric acid, 25DHBA contains only one carboxyl group and, additionally, two hydroxyl functions. Therefore, it is probably not surprising to find that in this case NTZ gave a cocrystal in 1:1 stoichiometry with the cocrystal former. NTZ-25DHBA-CH₃CN crystallized in the triclinic space group *P*1̄. The asymmetric unit comprises each one NTZ, 25DHBA and acetonitrile molecule, of which the latter was used as crystallization solvent. As in NTZ-SUC and NTZ-GLU, the COOH group of the now aromatic carboxylic acid is involved in a heterodimeric hydrogen bonding synthon with the carboxamide group of NTZ (motif V, Scheme 1b). The pendant OH groups in 25DHBA are involved in an intramolecular O–H…O hydrogen bond with the COOH group (2-OH group) and an intermolecular O–H…N bond with the acetonitrile solvate (5-OH group) (motifs VII and VIII in Scheme 1b) to give overall [1 + 1 + 1] aggregates (Figure 10).

Similar to NTZ-SUC and NTZ-GLU, within the crystal structure of NTZ-25DHBA-CH₃CN, the NTZ molecules are interconnected via two C–H…O and one π…π contact to give a 2D supramolecular structure with cavities which are occupied by 25DHBA·CH₃CN adducts (Figure 11). The NTZ network and the 25DHBA·CH₃CN adducts are linked via three C–H…O interactions, one O…C contact between the 5-OH group and the carbon of the NTZ amide group, and π-stacking between the thiazole unit of NTZ and the benzene ring of 25DHBA. Because of the latter interactions, the hydrogen-bonded NTZ-25DHBA complexes are stacked into 1D columns along *a* (Table S1, Figure 12).

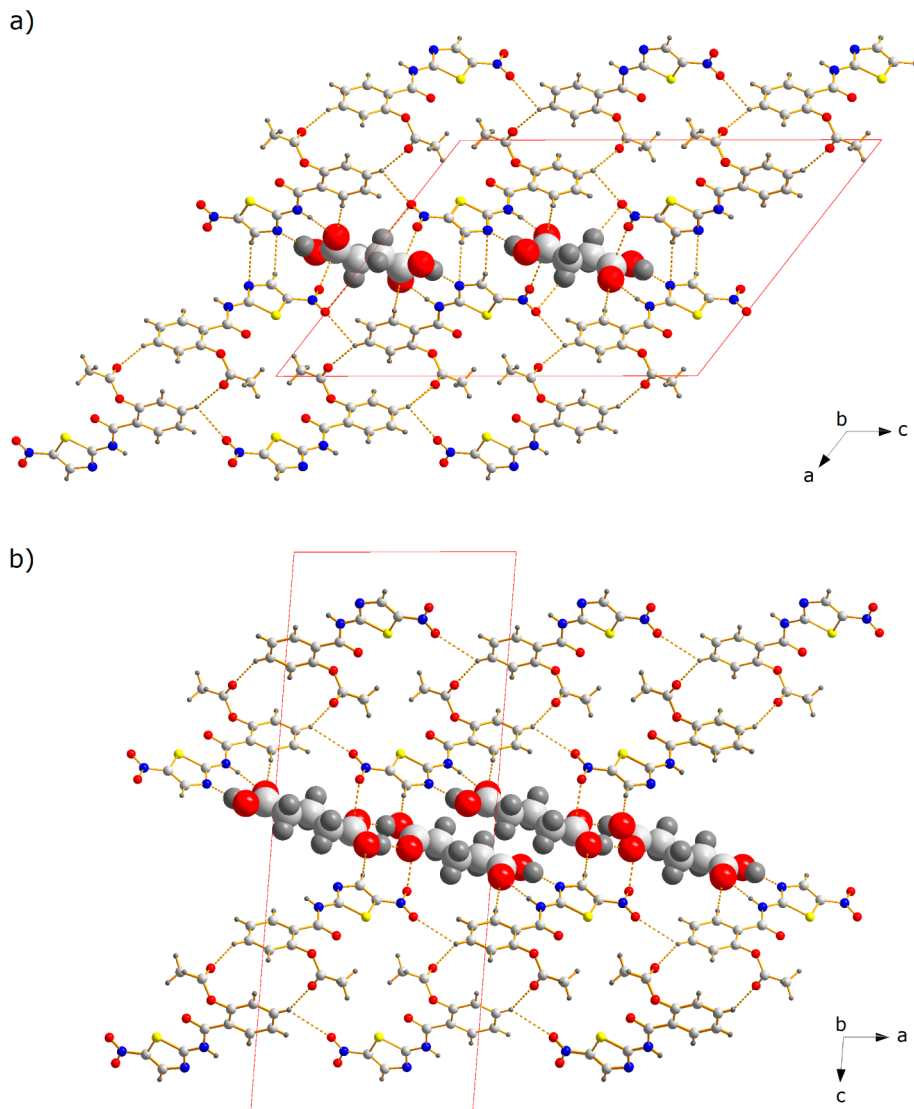


Figure 9. Fragments of the crystal structure of cocrystals (a) NTZ-SUC and (b) NTZ-GLU, showing the essential supramolecular connectivity.

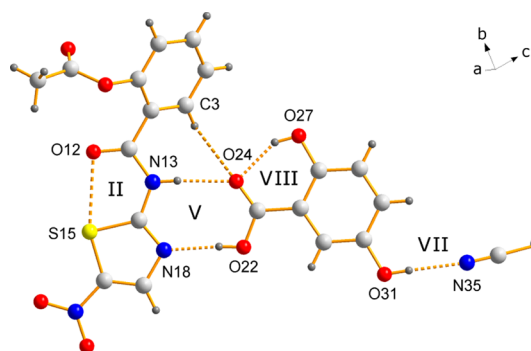


Figure 10. Fragment of the crystal structure of NTZ-2SDHBA-CH₃CN, showing the presence of [1 + 1 + 1] adducts between the components forming the cocrystal solvate.

Cocrystal versus Salt Formation. Analysis of the C–O distances of the single and double carbon–oxygen bonds in the carboxyl groups of the cocrystal formers in NTZ-SUC, NTZ-GLU, and NTZ-2SDHBA-CH₃CN allows us also to confirm that the new solid phases prepared herein are all pharmaceutical cocrystals and that salt formation did not take place. The

overview given in Table 7 shows that the C–O bond distances of 1.206(5)–1.225(3) Å for C=O and 1.311(4)–1.325(5) Å for C–O are found in the ranges established for neutral COOH groups (C–O: 1.3 Å and C=O: 1.2 Å). In the case of a carboxylate salt, the C–O bond lengths of the COO[−] group show a value intermediate between a single and a double bond (approximately 1.25 Å).^{13b,d,43}

3.5. Conformational Analysis of NTZ. NTZ possesses a relatively rigid molecular structure which is mostly planar. The coplanarity of the central thiazole ring and the attached salicylamide and nitro functions can be attributed to π -electron delocalization with the five-membered pseudoaromatic C₃NS ring. Further, NTZ has only restricted conformational flexibility because of two intramolecular noncovalent interactions, first an O···S contact which confines the structure to the Z-configuration and, second, an intramolecular N–H···OAc hydrogen bond (motifs I and II, Scheme 1a). Sperandeo and co-workers carried out solution and solid-state NMR studies of NTZ and, taking into account the single-crystal X-ray structure of NTZ, they evidenced that in solution (CDCl₃) and in the solid state it adopts the configuration and conformation given in Scheme 1a.¹⁵ However, in cocrystals NTZ-SUC, NTZ-GLU, and NTZ-

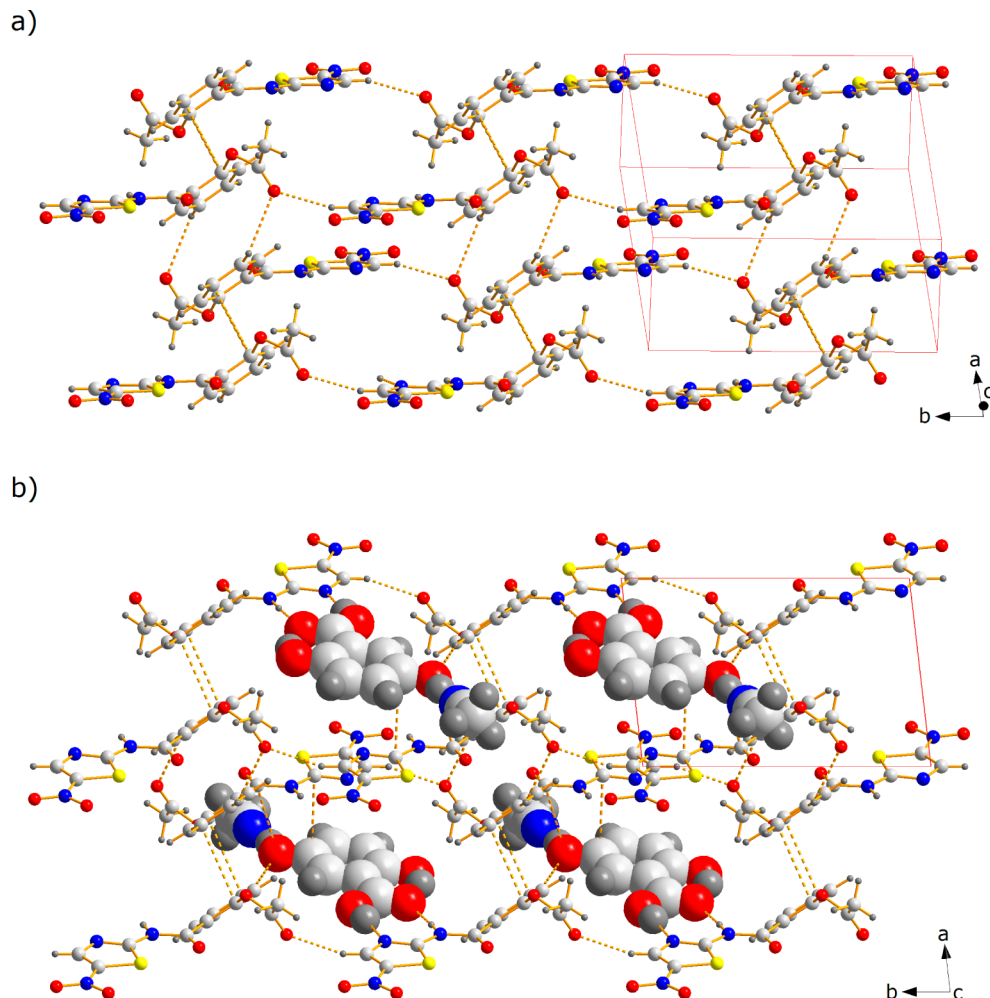


Figure 11. Fragments of the crystal structure of NTZ-2SDHBA-CH₃CN, showing the presence of 2D networks formed by NTZ molecules (a), whose cavities are filled by 2SDHBA-CH₃CN adducts (b).

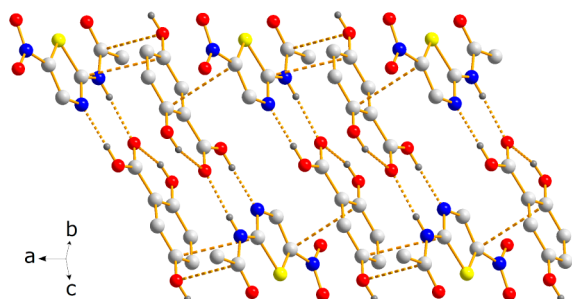


Figure 12. In NTZ-2SDHBA-CH₃CN, the complexes formed between NTZ and 2SDHBA are stacked into 1D columns along *a*. Note: For clarity, part of the atoms have been omitted.

Table 7. Bond Distances of the Carboxyl Groups in NTZ-SUC, NTZ-GLU, and NTZ-2SDHBA-CH₃CN

cocrystal	distance (Å) C–O	distance (Å) C=O
NTZ-SUC	1.325(5)	1.206(5)
NTZ-GLU	1.317(5)	1.206(5)
NTZ-2SDHBA-CH ₃ CN	1.311(4)	1.225(3)

2SDHBA-CH₃CN, the conformation of NTZ is changed, with the 2-(acetoxy)phenyl ring being now syn-oriented in relation to the C=O_{amide} function (Figure 13). The conformational change

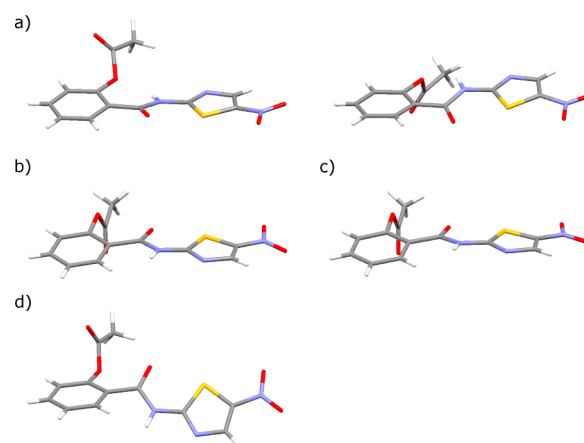


Figure 13. Comparative overview of the molecular conformations found in the crystal structures of (a) NTZ, (b) NTZ-SUC, (c) NTZ-GLU, and (d) NTZ-2SDHBA-CH₃CN.

enables a better availability of the functions participating in the formation of the heterodimeric hydrogen bonded synthon V with the COOH groups of the cocrystal former. Interestingly, the O···S interaction is conserved in all three cocrystals providing evidence for the structural importance of this contact. These findings are relevant also because the *N*-(1,3-thiazol-2-yl)-

Table 8. Geometrical Parameters for the Conformational Analysis of the NTZ Molecules in NTZ-SUC, NTZ-GLU, and NTZ-25DHB-CH₃CN^a

	configuration of OAc group ^b	C ₂ -C ₁ -O ₇ -C ₈ [°]	C ₁ -C ₂ -C ₁₁ -N ₁₃ [°]	C ₁₁ -N ₁₃ -C ₁₄ -S ₁₅ [°]	S ₁₅ -C ₁₆ -N ₁₉ -O ₂₀ [°]
NTZ ^c	anti	122.9(2) 118.0(2)	15.4(3) 15.2(3)	-8.6(3) -9.4(3)	-4.0(2) -3.5(2)
NTZ-SUC	syn	88.9(5)	172.3(4)	3.2(6)	7.1(6)
NTZ-GLU	syn	90.4(5)	169.5(3)	6.6(5)	3.6(5)
NTZ-25DHBA	syn	103.4(3)	142.4(3)	-3.2(4)	3.2(4)

^aAtom numbering is analogous to the chemical drawing of NTZ given in the introduction. ^bThe configuration is described in relationship to the C=O group. ^cData from ref 15, but atoms are numbered analogous to the NTZ molecules of the cocrystals described herein. The asymmetric unit comprises two crystallographically independent molecules.

carboxamide core is common to several important APIs having a spectrum of quite different pharmaceutical activities, that is, acetazolamide, AMG 517, aminitroxole, meloxicam, tenonitroxole, among others.

Table 8 summarizes some representative torsion angles for NTZ, NTZ-SUC, NTZ-GLU, and NTZ-25DHB-CH₃CN, of which the C₁₁-N₁₃-C₁₄-S₁₅ and S₁₅-C₁₆-N₁₉-O₂₀ torsion angles define the orientation of the amide and nitro groups in relation to the thiazole ring. The values for C₁-C₂-C₁₁-N₁₃ indicate the torsion of the salicyl aromatic ring regarding the amide group, and the values for C₂-C₁-O₇-C₈ describe the orientation of the acetoxy group. Comparison of the data compiled in Table 8 indicates major variations only for the orientation of the OAc group (C₂-C₁-O₇-O₈) and in the case of NTZ-25DHB-CH₃CN also for the C₁-C₂-C₁₁-N₁₃ torsion angle, indicating that for this compound the 2-(acetoxy)-benzeneamide fragment is significantly deviated from planarity. The panorama of the resulting conformers is visualized graphically in Figure 13.

4. BIOPHARMACEUTICAL EVALUATION OF NTZ-SUC AND NTZ-GLU

Because of low NTZ bioavailability, we examined some basic biopharmaceutically relevant properties to evaluate if the cocrystalline phases might be employed as alternative formulations with NTZ.

4.1. Phase Stability Tests. Indicative Stability. In this type of experiment, samples of each solid phase were exposed to standardized heat/humidity conditions to analyze if the phase was conserved or transformed into a two-phase mixture of NTZ and the cocrystal former. For the experiments, 30 mg of each NTZ-SUC, NTZ-GLU, and NTZ-25DHBA-CH₃CN were exposed for 30 days to the following stress conditions: (i) 40 °C, 0% RH, (ii) 50 °C, 0% RH, and (iii) 40 °C, 75% RH. After this period, the samples were examined by PXRD analysis, showing that both cocrystalline phases remained intact (Figures 14 and 15). On the contrary, NTZ-25DHBA-CH₃CN decomposed into a two-phase mixture of NTZ and 25DHBA, which can be attributed to the volatility of CH₃CN without which the cocrystalline structure is unstable.

Solution Phase Stability. Contrary to the indicative stability test, in this experiment the cocrystalline solid phases were exposed directly to (i) deionized water and aqueous solutions of two different compositions simulating physiological gastrointestinal conditions: (ii) 0.1 N HCl adjusted to pH 1.2, (iii) phosphate buffer, pH 7.5, 3% w/v CTAB. Because of the limited stability of the cocrystal solvate NTZ-25DHBA-CH₃CN in the former test, for the solution phase stability experiment only cocrystals NTZ-SUC and NTZ-GLU were employed. Figures 16 and 17 show the PXRD patterns of samples which have been

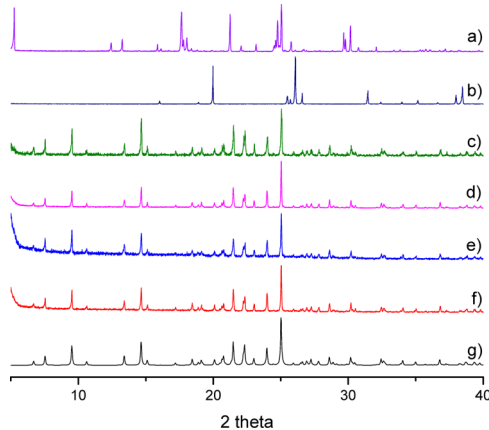


Figure 14. PXRD patterns of the following samples and experiments: (a) NTZ, (b) SUC, (c) sample of cocrystalline NTZ-SUC before indicative stability test, (d) sample of cocrystalline NTZ-SUC treated with dry heat at 40 °C, (e) sample of cocrystalline NTZ-SUC treated with dry heat at 50 °C, (f) sample of cocrystalline NTZ-SUC treated with heat at 40 °C and 75% RH, (g) pattern of NTZ-SUC simulated from the single-crystal X-ray diffraction analysis.

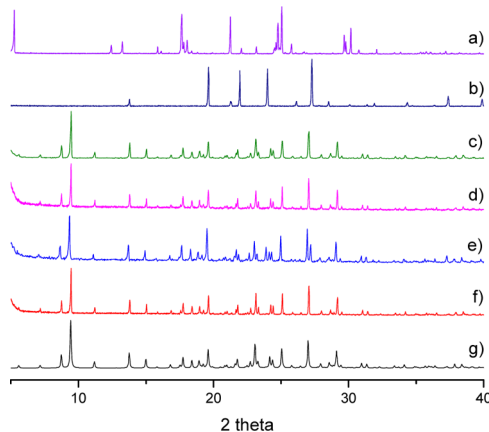


Figure 15. PXRD patterns of the following samples and experiments: (a) NTZ, (b) GLU, (c) sample of cocrystalline NTZ-GLU before indicative stability test, (d) sample of cocrystalline NTZ-GLU treated with dry heat at 40 °C, (e) sample of cocrystalline NTZ-GLU treated with dry heat at 50 °C, (f) sample of cocrystalline NTZ-GLU treated with heat at 40 °C and 75% RH, (g) pattern of NTZ-GLU simulated from the single-crystal X-ray diffraction analysis.

treated for 1 and 6 h with the above-mentioned solutions, indicating that decomposition into NTZ and the cocrystal former phase occurs in all cases already within 1 h.

4.2. Dissolution Rate. The measurement of the dissolution rates allows the intrinsic dissolution rate constants of cocrystals

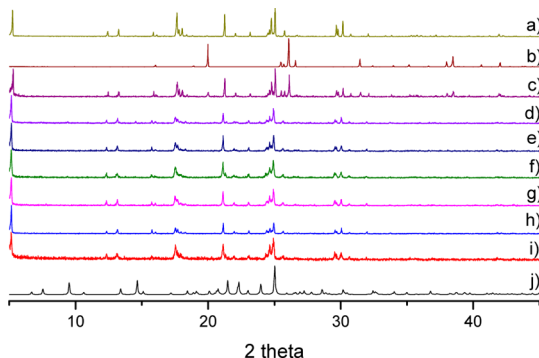


Figure 16. PXRD patterns of the following samples and experiments: (a) NTZ, (b) SUC, (c) physical mixture in 2:1 stoichiometry, (d) sample of cocrystalline NTZ-SUC stirred for 1 h in 0.1 N HCl, (e) sample of cocrystalline NTZ-SUC stirred for 1 h in deionized water, (f) sample of cocrystalline NTZ-SUC stirred for 1 h in phosphate buffer, pH 7.5 containing 3% w/v CTAB, (g) sample of cocrystalline NTZ-SUC stirred for 6 h in 0.1 N HCl, (h) sample of cocrystalline NTZ-SUC stirred for 6 h in deionized water, (i) sample of cocrystalline NTZ-SUC stirred for 6 h in phosphate buffer, pH 7.5 containing 3% w/v CTAB, (j) pattern of NTZ-SUC simulated from the single-crystal X-ray diffraction analysis.

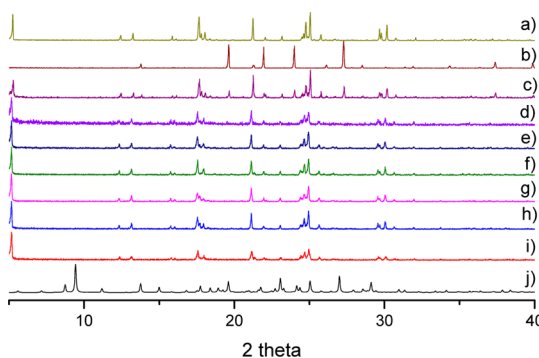


Figure 17. PXRD patterns of the following samples and experiments: (a) NTZ, (b) GLU, (c) physical mixture in 2:1 stoichiometry, (d) sample of cocrystalline NTZ-GLU stirred for 1 h in 0.1 N HCl, (e) sample of cocrystalline NTZ-GLU stirred for 1 h in deionized water, (f) sample of cocrystalline NTZ-GLU stirred for 1 h in phosphate buffer, pH 7.5 containing 3% w/v CTAB, (g) sample of cocrystalline NTZ-GLU stirred for 6 h in 0.1 N HCl, (h) sample of cocrystalline NTZ-GLU stirred for 6 h in deionized water, (i) sample of cocrystalline NTZ-GLU stirred for 6 h in phosphate buffer, pH 7.5 containing 3% w/v CTAB, (j) pattern of NTZ-GLU simulated from the single-crystal X-ray diffraction analysis.

NTZ-SUC and NTZ-GLU in comparison to NTZ to be established. The tests were performed using tablets of the cocrystals and NTZ, which were prepared with a hydraulic press at a total force of 30 kg/cm². The dissolution rates were determined with Wood's apparatus using a modified version of the dissolution conditions suggested by the Food and Drug Administration (phosphate buffer, pH 7.5, 3% w/v CTAB).⁴⁴ The experiments were carried out in triplicate at 37 °C under constant stirring (100 rpm). Samples were analyzed by UV-vis spectroscopy monitoring the absorption band at 435 nm (Figure S11, Supporting Information), which allowed us to quantify the amount of drug dissolved in a given time period and establish the dissolution rate profile. The comparative overviews given in Figure 18 and Table 9 show that there is a slight increase in the rate constants for NTZ-SUC (1.20-fold increase) and NTZ-

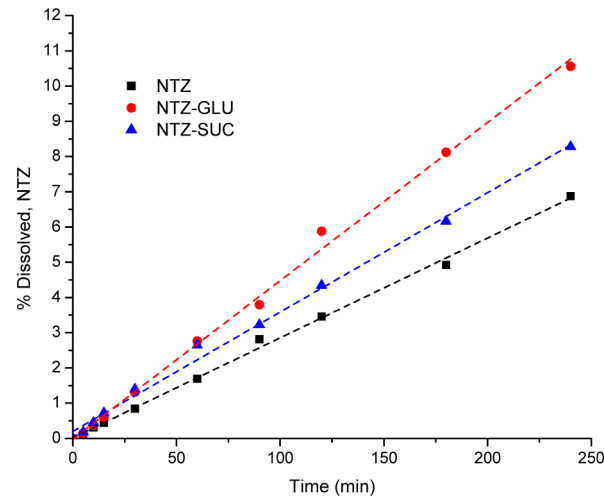


Figure 18. Dissolution profiles of NTZ, NTZ-SUC, and NTZ-GLU.

Table 9. Intrinsic Dissolution Rate Constants for NTZ, NTZ-SUC, and NTZ-GLU

	$K_{\text{intrinsic}}$ (% diss/min·cm ²)	$K_{\text{int}}(\text{cocrystal})/K_{\text{int}}(\text{NTZ})$
NTZ	0.06	1
NTZ-SUC	0.07	1.20
NTZ-GLU	0.09	1.59

GLU (1.59-fold increase). The small differences in comparison to pure NTZ are not surprising when taking into account that the cocrystalline phases are probably transformed into NTZ and cocrystal former during the dissolution experiment. Related surface-mediated transformation phenomena have been documented previously by the research groups of Shiraki,^{9d} Bogner,⁴⁵ and Childs.^{9p} PXRD analysis of the tablets formed with NTZ-SUC and NTZ-GLU before and after the dissolution rate experiments showed for both samples that part of the cocrystalline phase has decomposed into the phases of the individual components (Figures S12–S13, Supporting Information). This is in agreement with the results of the solution phase stability tests, which indicated that powders of the cocrystalline phases transform into a two-phase mixture of NTZ, and the cocrystal former when exposed to deionized water or solutions simulating physiological conditions at pH 1.2 and 7.5.

Previous studies by the research groups of Childs and Rodríguez-Hornedo suggest that cocrystals of APIs with coformers having at least 10 times higher water solubility than the underlying API will be more soluble than the pure API.^{9p,28a,46} Taking as reference the solubility of NTZ (7.6 µg/mL), all three coformers employed herein successfully for the formation of cocrystals with NTZ have a tremendously increased solubility (SUC, 58 g/L; GLU, 430 g/L; 2SDHBA, 5 g/L). In view of the observation that the dissolution rate experiments gave only relatively small increases when compared to pure NTZ, the generation of supersaturated conditions might be an option to obtain formulations with significantly enhanced intrinsic dissolution properties. Such supersaturated conditions can be accomplished with the addition of a solubilizing excipient (surfactant) and a polymeric precipitation inhibitor.^{9p}

4.3. Pressure Stability Tests. During the generation of the tablets required for the dissolution rate experiments, we observed that NTZ turned into liquid when treated with a hydraulic press at a total force of 40 kg/cm². Therefore, we examined the pressure stability of NTZ in comparison to cocrystals NTZ-SUC

and NTZ-GLU with the result that the latter did not become liquid within a pressure range of 30–60 kg/cm², while the solid phase of NTZ transformed to liquid starting from 40 kg/cm². The results are summarized in Table 10.

Table 10. Results of the Pressure Stability Tests for NTZ, NTZ-SUC, and NTZ-GLU

pressure	30 (kg/cm ²)	35 (kg/cm ²)	40 (kg/cm ²)	50 (kg/cm ²)	60 (kg/cm ²)
NTZ	solid	solid	liquid	liquid	liquid
NTZ-SUC	solid	solid	solid	solid	solid
NTZ-GLU	solid	solid	solid	solid	solid

5. CONCLUSIONS

This contribution has shown that it is possible to generate cocrystals of nitazoxanide using aliphatic or aromatic carboxylic acids. Interestingly, the cocrystals with the aliphatic acid homologues succinic and glutaric acid had different NTZ-cocrystal coformer stoichiometric ratios, NTZ-SUC 2:1 and NTZ-GLU 1:1.

Cocrystals NTZ-SUC and NTZ-GLU and the cocrystal solvate NTZ-2SDHBA-CH₃CN all showed a common heterodimeric supramolecular synthon formed between the carboxyl group of the cocrystal coformer and the carboxamidine fragment group of NTZ. Since this motif was predicted based on previous crystal engineering studies and on observations in other pharmaceutical cocrystals with carboxylic acids, it is evidenced that crystal engineering is indeed a helpful tool for the selection of potential cocrystal formers with a given API. Nevertheless, our success rate for cocrystal formation was only 10%, considering that a total of 29 carboxylic acids tested herein gave three cocrystalline phases. This rate is still too small in terms of a reliable performance of crystal engineering, and it is a major challenge to establish for each of the cocrystal formers the detailed reasons why cocrystal formation did occur or fail. It is evident that besides the primary synthon, secondary intermolecular interactions, that is, weaker noncovalent contacts and factors such as cooperativity in the supramolecular interactions and size compatibility between the molecular components, play an essential role in the molecular interplay that finally conduces either to a cocrystalline phase or crystallization in separate solid forms. Regarding the cocrystalline phases studied herein, this is somewhat illustrated by the following observations: (i) In the 2:1 complex with SUC, both COOH groups of the coformer participate in the formation of the COOH···HNNC synthon, while in the 1:1 complex with GLU, the coformer binds only one NTZ molecule each. The remaining COOH groups of GLU are involved in the formation of homodimeric COOH···HOOC synthons to give [2 + 2] aggregates that, interestingly, induce a similar supramolecular mutual organization of the NTZ molecules into 2D hydrogen bonded layers. This illustrates that the NTZ molecules have a propensity not only to form energetically favorable supramolecular synthons but also to achieve certain supramolecular interaction patterns that can be reached only if the coformer fulfills the required steric and binding properties. (ii) In NTZ-2SDHBA-CH₃CN, the NTZ molecules are organized in the form of a porous 2D supramolecular architecture in which adducts of 2SDHBA-CH₃CN are included in the cavities. In this case, only 2SDHBA interacts directly with NTZ, through the same synthon as observed above, and, apparently, the task of the solvent

molecules is to complement the size requirements of the coformer in order to fill the cavities in the inclusion complex.

The formation of heterodimeric synthons between the carboxamidine group of NTZ and the COOH groups of the cocrystal formers requires a conformational change of the molecular structure of NTZ. This isomerism implicates the rupture of the intramolecular N—H_{amide}···O_{OAc} bond found in pure NTZ but does not affect the intramolecular O···S interaction and shows that cocrystals can stabilize higher-energy molecular conformations of APIs allowing for their respective structural characterization.

Although they have different stoichiometric compositions (2:1 and 1:1), cocrystals NTZ-SUC and NTZ-GLU showed the same thermal behavior, starting with the loss of the cocrystal former, followed by decomposition of the remaining NTZ. This pattern is also followed by NTZ-2SDHBA-CH₃CN, which, however, previous to cocrystal former evaporation and NTZ degradation, presents desolvation of CH₃CN.

Although the pharmaceutical cocrystals NTZ-SUC and NTZ-GLU proved to be stable under indicative phase stability stress conditions (elevated temperature and humidity), they demonstrated to be unstable in aqueous solutions simulating physiological gastrointestinal conditions. Because of the low solution phase stability, it is likely to expect that the cocrystalline phases decomposed during the measurement of the dissolution rates with the result that the differences in relation to pure NTZ were negligible or only small. Nevertheless, the solid phases of cocrystals NTZ-SUC and NTZ-GLU showed better pressure stability when compared to NTZ, a finding that might be relevant for the pharmacotechnical specifications of this API.

This first study on cocrystals with NTZ opens the pathway for research projects on other combinations in the search of formulations showing better bioavailability of this highly insoluble drug.

■ ASSOCIATED CONTENT

Supporting Information

PXRD patterns for solid phases obtained from varying stoichiometric combinations of NTZ with GLU and SUC (2:1, 1:1, and 1:2). IR spectra for NTZ-SUC and NTZ-2SDHBA-CH₃CN. DSC-TG profiles for NTZ, NTZ-SUC, NTZ-GLU, and NTZ-2SDHBA-CH₃CN. Additional figures from the single-crystal X-ray diffraction analyses, and PXRD analysis of tablets for NTZ-SUC and NTZ-GLU before and after the dissolution rate determination. Table with additional intermolecular contacts in the crystal structures of NTZ-SUC, NTZ-GLU and NTZ-2SDHBA-CH₃CN. This information is available free of charge via the Internet at <http://pubs.acs.org/>.

■ AUTHOR INFORMATION

Corresponding Authors

*(D.H.-R.) E-mail: dherrera@uaem.mx.

*(H.H.) E-mail: hhopfl@uaem.mx.

Notes

The authors declare no competing financial interest.

■ ACKNOWLEDGMENTS

This work received financial support from Consejo Nacional de Ciencia y Tecnología (CONACyT) in the form of a postgraduate fellowship for BCFS and through Project No. CB2007-83440. We also thank Dr. Juan Pablo Senosiain Peláez, B. Sc. Gustavo Barranco Hernández, Dr. Efrén Hernández Baltazar, Dr. Jenniffer

Arenas-García, M. Sc. Juan Manuel Martínez Alejo, Dr. Virginia Montiel Palma, and Dr. Perla Román Bravo for their assistance in the characterization of the compounds described herein.

■ REFERENCES

- (1) (a) Despommier, D. D.; Gwadz, R. W.; Hotez, P. J., Eds.; *Parasitic Diseases*, 3rd ed.; Springer Verlag: New York, 1994. (b) Diarrhoea: Why children are still dying and what can be done. *UNICEF/WHO*: New York, 2009. (c) World Health Statistics, 2013.
- (2) Upcroft, P.; Upcroft, J. A. *Clin. Microbiol. Rev.* **2001**, *14*, 150–164.
- (3) (a) Rossignol, J. F.; Maisonneuve, H. *Am. J. Trop. Med. Hyg.* **1984**, *33*, S11–S12. (b) Rossignol, J. F.; Hidalgo, H.; Feregrino, M.; Higuera, F.; Gomez, W. H.; Romero, J. L.; Padierna, J.; Geyne, A.; Ayers, M. S. *Trans. R. Soc. Trop. Med. Hyg.* **1998**, *92*, 663–666. (c) Abaza, H.; Rahman El-Zayadi, A.; Kabil, S. M.; Rizk, H. *Curr. Ther. Res.* **1998**, *59*, 116–121. (d) Rossignol, J. F.; Ayoub, A.; Ayers, M. S. *Infect. Dis.* **2001**, *184*, 103–106. (e) Clinton, A. C., Jr. *Am. J. Trop. Med. Hyg.* **2003**, *68*, 382–383. (f) Diaz, E.; Mondragon, J.; Ramirez, E.; Bernal, R. *Am. J. Trop. Med. Hyg.* **2003**, *68*, 384–385. (g) Anderson, V. R.; Curran, M. P. *Drugs* **2007**, *67*, 1947–1967. (h) Schnyder, M.; Kohler, L.; Hemphill, A.; Deplazes, P. *Vet. Parasitol.* **2009**, *160*, 149–154. (i) Tritten, L.; Silbereisen, A.; Keiser, J. *Int. J. Parasitol.* **2012**, *2*, 98–105. (j) Hoffman, P. S.; Sisson, G.; Croxen, M. A.; Welch, K.; Harman, W. D.; Cremades, N.; Morash, M. G. *Antimicrob. Agents Chemother.* **2007**, *51*, 868–876.
- (4) For publications on modified NTZ derivatives see: (a) Ballard, T. E.; Wang, X.; Olekhovich, I.; Koerner, T.; Seymour, C.; Hoffman, P. S.; Macdonald, T. L. *Bioorg. Med. Chem. Lett.* **2010**, *20*, 3537–3539. (b) Navarrete-Vazquez, G.; Chávez-Silva, F.; Argotte-Ramos, R.; Rodríguez-Gutiérrez, M. C.; Chan-Bacab, M. J.; Cedillo-Rivera, R.; Moo-Puc, R.; Hernández-Núñez, E. *Bioorg. Med. Chem. Lett.* **2011**, *21*, 3168–3171.
- (5) (a) Rossignol, J.-F.; Abu-Zekry, M.; Hussein, A.; Santoro, M. G. *Lancet* **2006**, *368*, 124–129. (b) Korba, B. E.; Montero, A. B.; Farrar, K.; Gaye, K.; Mukerjee, S.; Ayers, M. S.; Rossignol, J. F. *Antivir. Res.* **2008**, *77*, S6–S63. (c) Teran, C. G.; Teran-Escalera, C. N.; Villarroel, P. *Int. J. Infect. Dis.* **2009**, *13*, 518–523. (d) Chan-Bacab, M. J.; Hernández-Núñez, E.; Navarrete-Vázquez, G. *J. Antimicrob. Chemother.* **2009**, *63*, 1292–1293. (e) Keeffe, E. B.; Rossignal, J. F. *World J. Gastroenterol.* **2009**, *15*, 1805–1808.
- (6) www.drugbank.ca/drugs/DB00507
- (7) Desiraju, G. R. *Angew. Chem., Int. Ed. Engl.* **1995**, *34*, 2311–2327.
- (8) For feature articles and reviews of pharmaceutical cocrystals see: (a) Almarsson, Ö.; Zaworotko, M. J. *Chem. Commun.* **2004**, 1889–1896. (b) Bernstein, J. *Chem. Commun.* **2005**, 5007–5012. (c) Vishweshwar, P.; McMahon, J. A.; Bis, J. A.; Zaworotko, M. J. *J. Pharm. Sci.* **2006**, *95*, 499–516. (d) Caira, M. R. *Mol. Pharmaceutics* **2007**, *4*, 310–316. (e) Blagden, N.; Berry, D. J.; Parkin, A.; Javed, H.; Ibrahim, A.; Gavan, P. T.; De Matos, L. L.; Seaton, C. C. *New J. Chem.* **2008**, *32*, 1659–1672. (f) Frischić, T.; Jones, W. *Cryst. Growth Des.* **2009**, *9*, 1621–1637. (g) Schultheiss, N.; Newman, A. *Cryst. Growth Des.* **2009**, *9*, 2950–2967. (h) Childs, S. L.; Zaworotko, M. J. *Cryst. Growth Des.* **2009**, *9*, 4208–4211. (i) Stahly, G. P. *Cryst. Growth Des.* **2009**, *9*, 4212–4229. (j) Upadhyay, N.; Shukla, T. P.; Mathur, A.; Manmohan; Jha, S. K. *Int. J. Pharm. Sci. Rev. Res.* **2011**, *8*, 144–148. (k) Babu, N. J.; Nangia, A. *Cryst. Growth Des.* **2011**, *11*, 2662–2679. (l) Brittain, H. G. *Cryst. Growth Des.* **2012**, *12*, 1046–1054. (m) Aitipamula, S.; Banerjee, R.; Bansal, A. K.; Biradha, K.; Cheney, M. L. *Cryst. Growth Des.* **2012**, *12*, 2147–2152. (n) Brittain, H. G. *Cryst. Growth Des.* **2012**, *12*, 5823–5832. (o) Thakuria, R.; Delori, A.; Jones, W.; Lipert, M. P.; Roy, L.; Rodríguez-Hornedo, N. *Int. J. Pharm.* **2013**, *453*, 101–125. (p) Brittain, H. G. *J. Pharm. Sci.* **2013**, *102*, 311–317. (q) Kelley, S. P.; Narita, A.; Holbrey, J. D.; Green, K. D.; Reichert, W. M.; Rogers, R. D. *Cryst. Growth Des.* **2013**, *13*, 965–975.
- (9) (a) McNamara, D. P.; Childs, S. L.; Giordano, J.; Iarricchio, A.; Cassidy, J.; Shet, M. S.; Mannion, R.; O'Donnell, E.; Park, A. *Pharm. Res.* **2006**, *23*, 1888–1897. (b) Variankaval, N.; Wenslow, R.; Murry, J.; Hartman, R.; Helmy, R.; Kwong, E.; Clas, S.-D.; Dalton, C.; Santos, I. *Cryst. Growth Des.* **2006**, *6*, 690–700. (c) Hickey, M. B.; Peterson, M. L.; Scoppettuolo, L. A.; Morrisette, S. L.; Vetter, A.; Guzmán, H.; Remenar, J. F.; Zhang, Z.; Tawa, M. D.; Haley, S.; Zaworotko, M. J.; Almarsson, Ö. *Eur. J. Pharm. Biopharm.* **2007**, *67*, 112–119. (d) Shiraki, K.; Takata, N.; Takano, R.; Hayashi, Y.; Terada, K. *Pharm. Res.* **2008**, *25*, 2581–2592. (e) Li, Z.; Yang, B.-S.; Jiang, M.; Eriksson, M.; Spinelli, E.; Yee, N.; Senanayake, C. *Org. Process Res. Dev.* **2009**, *13*, 1307–1314. (f) Takata, N.; Takano, R.; Uekusa, H.; Hayashi, Y.; Terada, K. *Cryst. Growth Des.* **2010**, *10*, 2116–2122. (g) Smith, A. J.; Kavuru, P.; Wojtas, L.; Zaworotko, M. J.; Shytle, R. D. *Mol. Pharm.* **2011**, *8*, 1867–1876. (h) Lee, H. G.; Zhang, G. G. Z.; Flanagan, D. R. *J. Pharm. Sci.* **2011**, *100*, 1736–1744. (i) Bethune, S. J.; Schultheiss, N.; Henck, J.-O. *Cryst. Growth Des.* **2011**, *11*, 2817–2823. (j) Rahman, Z.; Samy, R.; Sayeed, V. A.; Khan, M. A. *Pharm. Dev. Technol.* **2012**, *17*, 457–465. (k) Yan, Y.; Chen, J.-M.; Geng, N.; Lu, T.-B. *Cryst. Growth Des.* **2012**, *12*, 2226–2233. (l) Chadha, R.; Saini, A.; Jain, D. S.; Venugopalan, P. *Cryst. Growth Des.* **2012**, *12*, 4211–4224. (m) Sanphui, P.; Kumar, S. S.; Nangia, A. *Cryst. Growth Des.* **2012**, *12*, 4588–4599. (n) Lee, T.; Chen, H. R.; Lin, H. Y.; Lee, H. L. *Cryst. Growth Des.* **2012**, *12*, 5897–5907. (o) Billot, P.; Hosek, P.; Perrin, M.-A. *Org. Process Res. Dev.* **2013**, *17*, 505–511. (p) Childs, S. L.; Kandi, P.; Lingireddy, S. R. *Mol. Pharmacol.* **2013**, *10*, 3112–3127.
- (10) See for example the GRAS list. GRAS = Generally Regarded As Safe. This list is published by the U.S. Food and Drug Administration (FDA).
- (11) The pK_a value of the conjugated acid for the unsubstituted 1,3-thiazole, C₃H₃NS, is 2.44: Albert, A. In *Physical Methods in Heterocyclic Chemistry*; Katritzky, A. R., Ed.; Academic Press: New York, 1963; Vol. 1, Chapter 1.
- (12) Cheney, M. L.; Weyna, D. R.; Shan, N.; Hanna, M.; Wojtas, L.; Zaworotko, M. J. *Cryst. Growth Des.* **2010**, *10*, 4401–4413.
- (13) (a) Stahl, P. H.; Wermuth, C. G. In *Handbook of Pharmaceutical Salts: Properties, Selection, and Use*; Wiley-VCH: Zürich, 2002. (b) Bhogala, B. R.; Basavou, S.; Nangia, A. *CrystEngComm* **2005**, *7*, 551–562. (c) Delori, A.; Suresh, E.; Pedireddi, V. R. *Chem.—Eur. J.* **2008**, *14*, 6967–6977. (d) Childs, S. L.; Stahly, G. P.; Park, A. *Mol. Pharmaceutics* **2007**, *4*, 323–338.
- (14) (a) Cheney, M. L.; Weyna, D. R.; Shan, N.; Hanna, M.; Wojtas, L.; Zaworotko, M. J. *J. Pharm. Sci.* **2011**, *100*, 2172–2181. (b) Tumanov, N. A.; Myz, S. A.; Shakhtshneider, T. P.; Boldyreva, E. V. *CrystEngComm* **2012**, *14*, 305–313.
- (15) Bruno, F. P.; Caira, M. R.; Monti, G. A.; Kassuha, D. E.; Sperandeo, N. R. *J. Mol. Struct.* **2010**, *984*, 51–57.
- (16) Shikhar, K. G.; Soni Girish, C. J. S. K. *World J. Pharm. Pharm. Sci.* **2012**, *1*, 1344–1375.
- (17) Sherje, A. P.; Rahigude, A.; Warma, S.; Vanshiv, S. D. *Int. J. Chem. Tech. Res.* **2010**, *2* (4), 1966–1969.
- (18) Bansal, M. K.; Umashankar, M. S.; Gulati, M. *Inventi Impact: Pharm. Tech.* **2010**, *2010*, No. inventi:pt/34/10.
- (19) Espinosa-Lara, J. C.; Guzman-Villanueva, D.; Arenas-García, J. I.; Herrera-Ruiz, D.; Rivera-Islas, J.; Román-Bravo, P.; Morales-Rojas, H.; Höpfel, H. *Cryst. Growth Des.* **2013**, *13*, 169–185.
- (20) (a) Shan, N.; Toda, F.; Jones, W. *Chem. Commun.* **2002**, 2372–2373. (b) Trask, A. V.; Motherwell, W. D. S.; Jones, W. *Chem. Commun.* **2004**, 890–891.
- (21) Recently, instead of “solvent drop grinding” the term “liquid-assisted grinding” is frequently used: Frischić, T.; Trask, A. V.; Jones, W.; Motherwell, W. D. S. *Angew. Chem., Int. Ed.* **2006**, *45*, 7546–7550.
- (22) (a) Zhang, G. G. Z.; Henry, R. F.; Borchardt, T. B.; Lou, X. J. *Pharm. Sci.* **2007**, *96*, 990–995. (b) Takata, N.; Shiraki, K.; Takano, R.; Hayashi, Y.; Terada, K. *Cryst. Growth Des.* **2008**, *8*, 3032–3037.
- (23) Rodríguez-Hornedo, N.; Nehm, S. J.; Seefeldt, K. F.; Pagán-Torres, Y.; Falkiewicz, C. J. *Mol. Pharmaceutics* **2006**, *3*, 362–367.
- (24) (a) SMART: *Bruker Molecular Analysis Research Tool*, Versions 5.057 and 5.0618, Bruker Analytical X-ray Systems: Karlsruhe, Germany, 1997 and 2000. (b) SAINT + NT, Versions 6.01 and 6.04; Bruker Analytical X-ray Systems: Karlsruhe, Germany, 1999 and 2001. (c) Sheldrick, G. M. *SHELX86, Program for Crystal Structure Solution*; University of Göttingen: Germany, 1986. (d) *SHELXTL-NT*, Versions

- S.10 and 6.10; Bruker Analytical X-ray Systems: Karlsruhe, Germany, 1999 and 2000.
- (25) Farrugia, L. J. *J. Appl. Crystallogr.* **1999**, *32*, 837–838.
- (26) Brandenburg, K. *Diamond*, version 3.1c; Crystal Impact: University of Bonn, 1997.
- (27) (a) Stanton, M. K.; Bak, A. *Cryst. Growth Des.* **2008**, *8*, 3856–3862. (b) Stanton, M. K.; Kelly, R. C.; Colletti, A.; Langley, M.; Munson, E. J.; Peterson, M. L.; Roberts, J.; Wells, M. *J. Pharm. Sci.* **2011**, *100*, 2734–2743.
- (28) (a) Childs, S. L.; Rodríguez-Hornedo, N.; Reddy, L. S.; Jayasankar, A.; Maheshwari, C.; McCausland, L.; Shippert, R.; Stahly, B. C. *CrystEngComm* **2008**, *10*, 856–864. (b) Childs, S. L.; Wood, P. A.; Rodríguez-Hornedo, N.; Reddy, L. S.; Hardcastle, K. I. *Cryst. Growth Des.* **2009**, *9*, 1869–1888.
- (29) (a) Remenar, J. F.; Morissette, S. L.; Peterson, M. L.; Moulton, B.; MacPhee, J. M.; Guzmán, H. R.; Almarsson, Ö. *J. Am. Chem. Soc.* **2003**, *125*, 8456–8457. (b) Lahtinen, M.; Kolehmainen, E.; Haarala, J.; Shevchenko, A. *Cryst. Growth Des.* **2013**, *13*, 346–351.
- (30) Childs, S. L.; Hardcastle, K. I. *Cryst. Growth Des.* **2007**, *7*, 1291–1304.
- (31) (a) Trask, A. V.; Motherwell, W. D. S.; Jones, W. *Int. J. Pharm.* **2006**, *320*, 114–123. (b) Zhang, S.; Rasmuson, A. C. *Cryst. Growth Des.* **2013**, *13*, 1153–1161.
- (32) (a) Aitipamula, S.; Chow, P. S.; Tan, R. B. H. *CrystEngComm* **2009**, *11*, 1823–1827. (b) Liao, X.; Gautam, M.; Grill, A.; Zhu, H. J. *J. Pharm. Sci.* **2010**, *99*, 246–254. (c) Kastelic, J.; Hodnik, Ž.; Šket, P.; Plavec, J.; Lah, N.; Leban, I.; Pajk, M.; Planinšek, O.; Kikelj, D. *Cryst. Growth Des.* **2010**, *10*, 4943–4953. (d) Martin, F. A.; Pop, M. M.; Borodi, G.; Filip, X.; Kacso, I. *Cryst. Growth Des.* **2013**, *13*, 4295–4304.
- (33) (a) Arenas-García, J. I.; Herrera-Ruiz, D.; Mondragon-Vasquez, K.; Morales-Rojas, H.; Höpfl, H. *Cryst. Growth Des.* **2010**, *10*, 3732–3742. (b) Arenas-García, J. I.; Herrera-Ruiz, D.; Mondragon-Vasquez, K.; Morales-Rojas, H.; Höpfl, H. *Cryst. Growth Des.* **2012**, *12*, 811–824.
- (34) (a) Brittain, H. G. *Cryst. Growth Des.* **2009**, *9*, 2492–2499. (b) Brittain, H. G. *Cryst. Growth Des.* **2009**, *9*, 3497–3503. (c) Brittain, H. G. *Cryst. Growth Des.* **2010**, *10*, 1990–2003.
- (35) (a) Ángyán, J. G.; Poirier, R. A.; Kucsman, A.; Csizmadia, I. G. *J. Am. Chem. Soc.* **1987**, *109*, 2237–2245. (b) Pandya, N.; Basile, A. J.; Gupta, A. K.; Hand, P.; MacLaurin, C. I.; Mohammad, T.; Ratemi, E. S.; Gibson, M. S.; Richardson, M. F. *Can. J. Chem.* **1993**, *71*, 561–571. (c) Minkin, V. I.; Minyaev, R. M. *Chem. Rev.* **2001**, *101*, 1247–1265. (d) Nagao, Y.; Honjo, T.; Iimori, H.; Goto, S.; Sano, S.; Shiro, M.; Yamaguchi, K.; Sei, Y. *Tetrahedron Lett.* **2004**, *45*, 8757–8761. (e) Bleiholder, C.; Werz, D. B.; Köppel, H.; Gleiter, R. *J. Am. Chem. Soc.* **2006**, *128*, 2666–2674. (f) Nakanishi, W.; Nakamoto, T.; Hayashi, S.; Sasamori, T.; Tokito, N. *Chem.—Eur. J.* **2007**, *13*, 255–268. (g) Hayashi, K.; Ogawa, S.; Sano, S.; Shiro, M.; Yamaguchi, K.; Sei, Y.; Nagao, Y. *Chem. Pharm. Bull.* **2008**, *56*, 802–806. (h) Milov, A. A.; Minyaev, R. M.; Minkin, V. I. *J. Phys. Chem. A* **2011**, *115*, 12973–12982. (i) Navarrete-Vázquez, G.; Alaniz-Palacios, A.; Tlahuextl, M.; Bernal-Uruchurtu, M.; Tlahuext, H. *CrystEngComm* **2012**, *14*, 1256–1263.
- (36) (a) Allen, F. H.; Motherwell, W. D. S.; Raithby, P. R.; Shields, G. P.; Taylor, R. *New J. Chem.* **1999**, *25*–34. (b) Bensemann, I.; Gdaniec, M.; Polonski, T. *New J. Chem.* **2002**, *26*, 448–456. (c) Bis, J. A.; Zawarotko, M. J. *Cryst. Growth Des.* **2005**, *5*, 1169–1179. (d) Thompson, L. J.; Elias, N.; Male, L.; Tremayne, M. *Cryst. Growth Des.* **2013**, *13*, 1464–1472.
- (37) Tao, Q.; Chen, J.-M.; Ma, L.; Lu, T.-B. *Cryst. Growth Des.* **2012**, *12*, 3144–3152.
- (38) Allen, F. H. *Acta Crystallogr.* **2002**, *B58*, 380–388.
- (39) (a) Chiarella, R. A.; Davey, R. J.; Peterson, M. L. *Cryst. Growth Des.* **2007**, *7*, 1223–1226. (b) ter Horst, J. H.; Cains, P. W. *Cryst. Growth Des.* **2008**, *8*, 2537–2542. (c) Jayasankar, A.; Reddy, L. S.; Bethune, S. J.; Rodríguez-Hornedo, N. *Cryst. Growth Des.* **2009**, *9*, 889–897.
- (40) Stanton, M. K.; Tufekcic, S.; Morgan, C.; Bak, A. *Cryst. Growth Des.* **2009**, *9*, 1344–1352.
- (41) (a) Mukherjee, G.; Biradha, K. *Cryst. Growth Des.* **2011**, *11*, 924–929. (b) Torres-Huerta, A.; Höpfl, H.; Tlahuext, H.; Hernández-Ahuactzi, I. F.; Sánchez, M.; Reyes-Martínez, R.; Morales-Morales, D. *Eur. J. Inorg. Chem.* **2013**, 61–69. (c) Jelfs, K. E.; Eden, E. G. B.; Culshaw, J. L.; Shakespeare, S.; Pyzer-Knapp, E. O.; Thompson, H. P. G.; Bacsa, J.; Day, G. M.; Adams, D. J.; Cooper, A. *I. J. Am. Chem. Soc.* **2013**, *135*, 9307–9310.
- (42) Tothadi, S.; Desiraju, G. R. *Cryst. Growth Des.* **2012**, *12*, 6188–6198.
- (43) Bis, J. A.; Zawarotko, M. J. *Cryst. Growth Des.* **2005**, *5*, 1169–1179.
- (44) For NTZ, the FDA-recommended dissolution method refers to the following conditions: phosphate buffer pH = 7.5, T = 37 °C and 6% w/v CTAB. Since we observed that CTAB started to precipitate under these conditions, we performed a series of solubility tests for NTZ in the above-mentioned medium but varying the CTAB concentration gradually from 1 to 6%. Since the degree of solubilization did not vary significantly in the CTAB range from 3 to 6%, we decided to complete the dissolution rate determinations for NTZ and cocrystals NTZ-GLU and NTZ-SUC at the following modified conditions: Phosphate buffer pH = 7.5, T = 37 °C, and 3% w/v CTAB.
- (45) Greco, K.; Bogner, R. *J. Pharm. Sci.* **2012**, *101*, 2996–3018.
- (46) Good, D. J.; Rodríguez-Hornedo, N. *Cryst. Growth Des.* **2009**, *9*, 2252–2264.